

## **Design of a Single Stage Axial Flow Turbine**



**Case Western Reserve University**

**Department of Aerospace and Mechanical Engineering**

Designed by:

William Koehrsen

Tyler Eston

Arturo Garcia

Theodore Bastian

**EMAE 355 Project #3**

**Professor**

Dr. J.R. Kadambi

**Teaching Assistant**

Scott Rubeo

November 18, 2017

## Abstract

---

This report details the design of a single stage axial flow turbine for use in a small turbojet engine. According to [1], this turbine must operate at the same shaft speed, 250 rev/sec, as the compressor in the engine and have a blade speed of 340 m/s based upon previous turbine design experience. The inlet stagnation temperature and pressure of the turbine were fixed from the cycle calculations for the engine as was the stagnation temperature drop and stagnation pressure ratio across the turbine. The turbine was designed for an air mass flow rate of 20 kg/s while operating at an isentropic efficiency of 0.91. Losses for the turbine were to be taken into account in the initial design by means of the overall isentropic efficiency as well as an estimated nozzle loss coefficient of 0.05. The final requirement for the turbine was that the exit Mach number of the flow not exceed 0.6.

The turbine was designed based on empirical data and a set of velocity triangles with a stated design goal of a 50% reaction. The flow coefficient for the turbine was selected based on experimental data to be 0.8 which meant that an absolute rotor exit angle,  $\alpha_3$ , of  $16^\circ$  resulted in the reaction closest to 50%. This angle selection drove the rest of the absolute and relative angles and velocities throughout the turbine, which ultimately constrained the physical dimensions for the turbine. The annulus area at station 1, the inlet to the nozzle, is  $0.0621 \text{ m}^2$ ; the annulus area at station 2, the exit of the nozzle and entrance to the rotor, is  $0.0785 \text{ m}^2$ ; and the annulus area at station 3, the exit of the rotor, is  $0.1047 \text{ m}^2$ . These areas determined the dimensions of the blades and diameters. The average nozzle blade height is 0.0517 m and the average rotor blade height is 0.0674 m. The mean radius is 0.216 m, the average nozzle hub radius is 0.191 m, the average nozzle tip radius is 0.242 m, the average rotor hub radius is 0.183 m, and the average rotor tip radius is 0.250 m. The final turbine stage had a Mach number at the exit of the rotor of 0.476, below the maximum allowed as determined by [1] and the flow remains subsonic throughout the stage. In the stator row there are 34 blades, and in the rotor row there are 26 blades. The isentropic efficiency achieved by the turbine is 87.6% which was judged to be within an acceptable range of the specifications. The turbine stage meets all the prescribed design requirements and accounting for the 20 kg/s mass flow rate in the problem specifications, the turbine will produce 3.329 MW of shaft work. The turbine blades will be made out of cobalt and will be manufactured using investment casting. The approximate cost to produce the blades in the turbine is \$4600.

## Table of Contents

---

Section 1: Introduction.....	2
Section 2: Nomenclature.....	3
Section 3: Methods .....	6
3.1 Assumptions .....	6
3.2 Design Procedure .....	7
3.3 Selection of Parameters .....	19
Section 4: Results.....	22
4.1 Specifications .....	22
4.2 Velocity Triangles and Turbine Diagram.....	25
4.3 Bill of Materials and Cost Analysis .....	27
Section 5: Discussion.....	29
5.1 Design Justification .....	29
5.2 Alternative Designs .....	31
Section 6: Conclusion .....	33
Section 7: Acknowledgements.....	34
Section 8: References.....	35
Section 9: Academic Integrity Statement .....	36
Section 10: Appendices.....	37

## Section 1: Introduction

---

In order to facilitate the development of a small turbojet engine, a single stage turbine was designed in alignment with conditions determined by the engine cycle calculations. The relevant requirements were outlined in [1], the most crucial of which are that the turbine operates with a shaft rotational speed of 250 rev/sec, a mean blade speed of 340 m/s, and an isentropic efficiency of 0.91. The cycle calculations also provided a set of temperature and pressure constraints for the turbine. The losses for the turbine stage were to be taken into account by means of the overall isentropic efficiency as well as an estimated nozzle loss coefficient. In addition to the cycle calculations, specifications for the turbine were based on previous turbine development experience. The final design of the turbine was to include velocity triangles, annulus flow areas, mean, tip, and hub radii, blade heights, and the number of blades in the nozzle and the rotor. Empirical data was heavily relied upon in the design of the single stage turbine and proved essential in the selection of several critical parameters.

## Section 2: Nomenclature

---

- Throughout the report, the terms nozzle and stator are used interchangeably
- The subscript 1 refers to station 1, the inlet to the nozzle
- The subscript 2 refers to station 2, the outlet of the nozzle and inlet to the rotor
- The subscript 3 refers to station 3, the exit of the rotor
- The subscript  $x$  refers to the axial direction and  $\theta$  refers to the tangential direction
- The subscript 0 on a state property refers to the stagnation value while state properties with no subscript refer to the static value
- The subscript  $s$  refers to the stator (nozzle) row and subscript  $r$  refers to the rotor row
- The subscript  $h$  refers to the hub,  $t$  refers to the tip, and  $m$  refers to the mean dimension
- The superscript ' refers to the isentropic value of a state property
- The absolute angles,  $\alpha$ , are the angles between the axial velocity and the absolute velocity
- The relative angles,  $\beta$ , are the angles between the axial velocity and the relative velocity

Symbol	Description	Units
$A$	Area	$\text{m}^2$
$AR$	Turbine blade aspect ratio	-
$b$	Blade axial chord	m
$c_p$	Specific heat capacity at constant pressure for air	J/ kg K
$C$	Absolute flow velocity	m/s
$C_x$	Axial absolute flow velocity	m/s
$C_\theta$	Tangential absolute flow velocity	m/s
$D_h$	Hydraulic Diameter	m
$h$	Turbine blade height	m
$h_t$	Enthalpy at station 1	J/kg
$Ma$	Mach number	-
$\dot{m}$	Mass flow rate	kg/s
$n$	Number of turbine blades	-
$P$	Static Pressure	kPa

$P_0$	Stagnation pressure	kPa
$R$	Specific gas ratio for air	J/kg K
$R_N$	Engine blade stage reaction	-
$Re_D$	Reynolds number	-
$r_h$	Hub radius	m
$r_t$	Tip radius	m
$r_m$	Mean radius	m
$s$	Turbine blade pitch	m
$T$	Static Temperature	K
$T'$	Isentropic static temperature	K
$T_0$	Stagnation temperature	K
$U$	Mean blade speed	m/s
$w$	Relative flow velocity	m/s
$\dot{W}$	Work output	W
$\dot{w}$	Work rate per unit mass flow	m <sup>2</sup> /s <sup>2</sup>
$\alpha$	Absolute angle	°
$\beta$	Relative angle	°
$\gamma$	Specific heat ratio	-
$\eta_T$	Design Isentropic efficiency	-
$\eta_{T,a}$	Achieved Isentropic efficiency	-
$\lambda_N$	Estimated Nozzle loss coefficient	-
$\zeta^*$	Preliminary energy loss coefficient	-
$\zeta_S$	Nozzle energy loss coefficient	-
$\zeta_R$	Rotor energy loss coefficient	-

$\rho$	Density	kg/m <sup>3</sup>
$\psi$	Stage loading (work) coefficient	-
$\varphi$	Flow coefficient	-
$\Omega$	Rotational speed of shaft	rev/sec

## Section 3: Methods

---

### 3.1 Assumptions

- Air behaves as an ideal gas throughout the turbine stage. This allows the state properties at the three stations to be calculated using the ideal gas equation of state and the definition of stagnation properties.
- The specific heat of air and the specific heat ratio of the air are constant throughout the turbine.
- The nozzle does not produce any work. This means that the stagnation temperature at station 1 will be equal to the stagnation temperature at station 2.
- The turbine will operate at a steady state. This simplifies the analysis and design of the turbine as the equations are not time-dependent.
- Losses through the turbine stage are accounted for by means of the overall isentropic efficiency,  $\eta_T$ , and the nozzle loss coefficient,  $\lambda_N$ . The losses could alternatively be accounted for with a nozzle loss coefficient and then a rotor loss coefficient but this approach was not utilized in the design. However, this approach was used to calculate the achieved isentropic efficiency after the design had been completed.
- Mean blade speed as specified in the design requirements was constant throughout the turbine.
- The axial velocity of the air flow throughout the turbine is constant and the air flow enters the turbine stage axially.
- Air does not react with the cobalt of the turbine blades according to the Material Safety Data Sheet for Cobalt [2].
- Empirical data was heavily relied upon in the design of the turbine stage. The data was assumed to be accurate and applicable to the development of a small turbine.



### 3.2 Design Procedure

Numerous approaches can be utilized in the design of a single stage axial flow turbine. The approach employed in this design employed empirical turbine data to achieve a desired isentropic efficiency based on the problem specifications.

#### *Problem Specifications*

The design specifications for the turbine be derived are outlined in [1] and shown in Table 1.

Description	Value	Units
Mass flow rate, $\dot{m}$	20	kg/s
Isentropic efficiency, $\eta_T$	0.91	-
Inlet stagnation temperature, $T_{01}$	1103.15	K
Stagnation temperature drop, $T_{01} - T_{03}$	145	K
Stagnation pressure ratio ( $P_{01}/P_{03}$ )	1.9	-
Inlet stagnation pressure, $P_{01}$	410	kPa
Rotational speed of shaft, $\Omega$	250	rev/sec
Mean blade speed, $U$	340	m/s
Estimated Nozzle loss coefficient, $\lambda_N$	0.05	-
Specific gas constant for air, $R$	287	J/kg K
Heat capacity of air, $c_p$	1148	J/ kg K
Specific heat ratio (adiabatic index), $\gamma$	1.333	-
Maximum exit Mach number	0.6	-

**Table 1: Design Specifications for Turbine from [1]**

### Velocity Triangles

Velocity triangles were used extensively to facilitate the design of the turbine. The symbolic velocity triangles are shown in Figure 1 for reference.

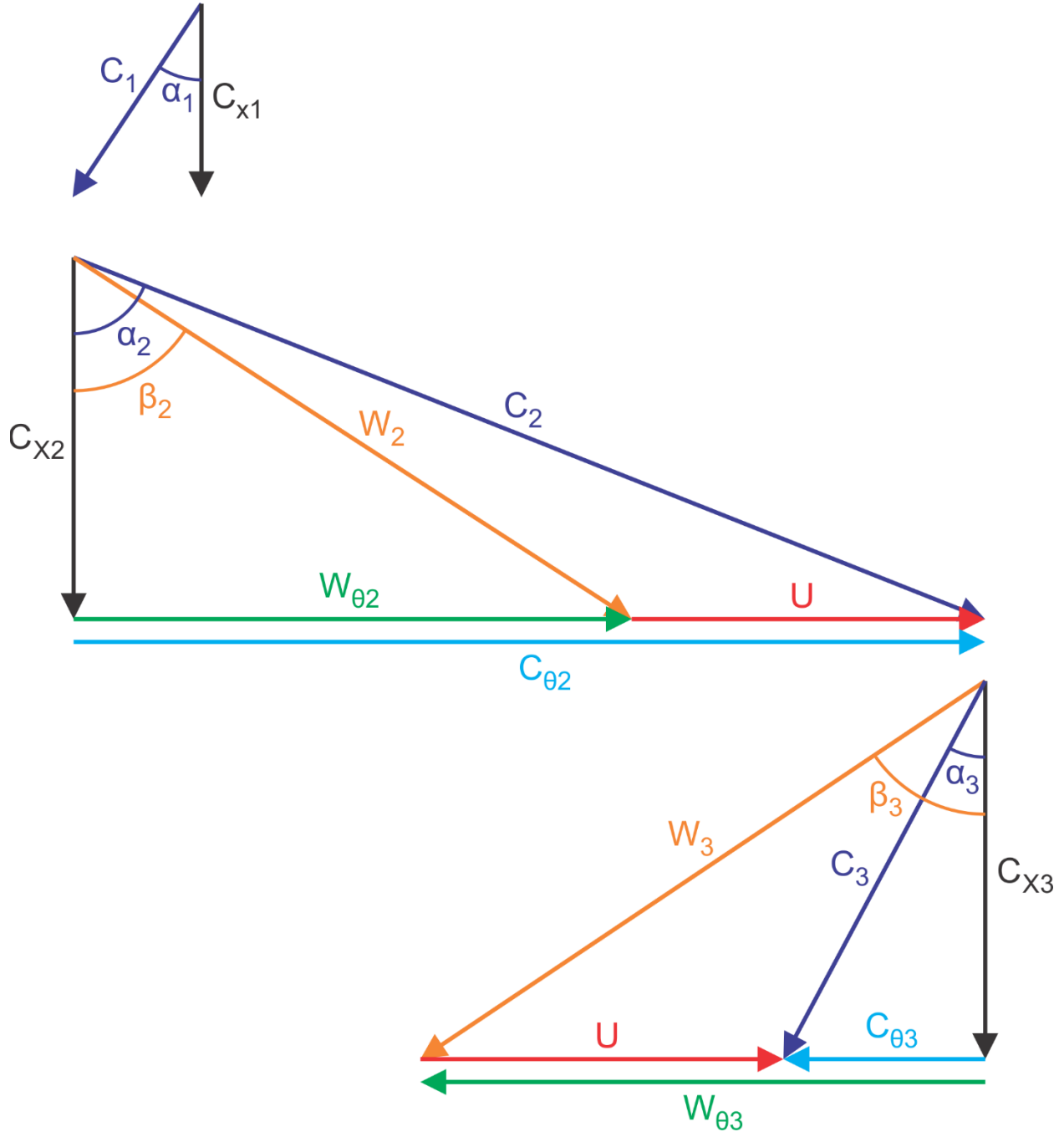


**Figure 1: Symbolic Velocity Triangles**

### *Station Definition*

Three separate stations were defined to facilitate the design of the turbine. Station 1 is the inlet flow entering the nozzle, 2 is the flow exiting the nozzle and entering into the rotor, and 3 is the flow exiting the rotor row. The schematic of the turbine stage is shown in Figure 2.

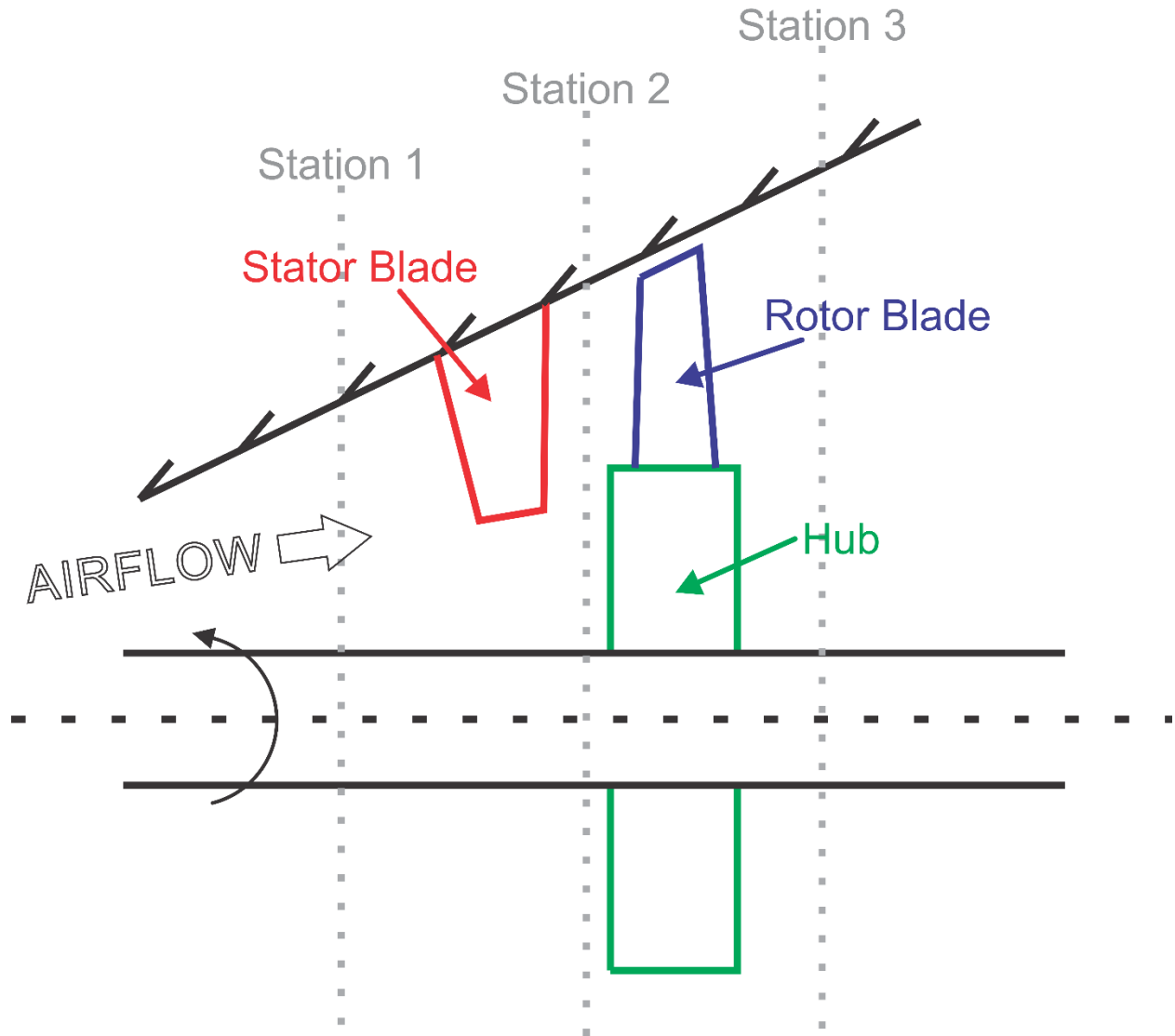


**Figure 2: Turbine Stage Schematic**

### ***Velocity Suppositions***

Several import conclusions regarding the velocities through the turbine stage were made from arguments presented in [3] and [4] based on the principles of single stage turbomachinery. These conclusions proved crucial to the design process and are shown in Table 2.

<b>Description</b>	<b>Symbolic Notation</b>
Mean blade speed is constant throughout stage	$U_2 = U_3 = U$
Axial velocity through stage is constant	$C_{x,1} = C_{x,2} = C_{x,3} = C_x$
Flow enters turbine axially	$\alpha_1 = 0, C_{x,1} = C_1$

**Table 2: Velocity Conclusions**

### ***Dimensionless Parameters***

From the specifications, several critical parameters can be calculated.  $\psi$ , the stage loading coefficient, (also known as the work coefficient) is one of three dimensionless parameters used to characterize the turbine stage. The definition of  $\psi$  is provided on page 19 of [3]:

$$\psi = \frac{\Delta W}{U^2} = \frac{c_p * \Delta T_0}{U^2} \quad (1)$$

Where  $\Delta W$  is the work per unit mass flow rate in  $\text{m}^2/\text{s}^2$ ,  $U$  is the mean blade velocity in  $\text{m/s}$ ,  $c_p$  is the heat capacity of air in  $\text{J/kg K}$ , and  $\Delta T_0$  is the stagnation temperature drop across the turbine in  $\text{K}$ . The next dimensionless number to determine was  $\phi$ , the flow coefficient. The flow coefficient is defined on page 19 of [3]:

$$\phi = \frac{C_x}{U} \quad (2)$$

Where  $C_x$  is the axial flow velocity which is assumed to be constant for an axial turbine. However,  $C_x$  was not provided in the design specifications, which meant that the flow coefficient must be determined from empirical data. Figure 4.11 on page 119 of [4] provides a graph of stage loading coefficient,  $\psi$ , versus flow coefficient,  $\phi$ , with contours drawn at differing isentropic efficiencies. This chart is based on experimental studies on turbines undertaken by Rolls Royce and published in the Royal Aeronautical Society Journal. As both the stage loading coefficient and the desired isentropic efficiency are known, the flow coefficient experimentally corresponding to these parameters can be selected from the chart. The third dimensionless parameter, and the final one needed to characterize the turbine, is the stage reaction. This is defined on page 101 of [4] as the ratio of the static enthalpy drop across the rotor to the static enthalpy drop across the stage:

$$R_N = \frac{h_{t,2} - h_{t,3}}{h_{t,1} - h_{t,3}} \quad (3)$$

The reaction can also be characterized in terms of the flow coefficient assuming the absolute velocity entering the nozzle row equals the absolute velocity exiting the rotors according to page 20 of [3]:

$$R_N = \frac{\varphi}{2} (\tan \beta_3 - \tan \beta_2) \quad (4)$$

Where  $\beta_3$  is the angle between the relative velocity and the axial velocity exiting the rotor and  $\beta_2$  is the angle between the relative velocity and the axial velocity exiting the nozzle. The  $\beta$  angles are referred to as the relative angles (with  $\beta_2$  the nozzle relative angle and  $\beta_3$  the rotor relative angle) and the  $\alpha$  angles are referred to as the absolute angles.

The next step was to select a rotor absolute angle,  $\alpha_3$ , for the turbine. Although a multi-stage turbine generally has the incoming flow angle and the outlet flow angle equal to zero,  $\alpha_1 = \alpha_3 = 0$ , meaning that the flow enters and exits axially, for a single stage turbine this condition does not have to be satisfied according to [5]. The inlet flow was selected to be axial, but the rotor absolute angle,  $\alpha_3$ , was varied to observe the effects on the reaction of the turbine and to maximize the efficiency of the turbine. The angle for the outlet flow was ultimately driven by the design goal of a 50% reaction. The reasons for selecting a 50% reaction for a turbine stage are outlined on pages 110-115 of [4] and are described in detail in the Discussion section of this report.

Designing for a reaction of 50% meant calculating the reaction value for a range of  $\alpha_3$  values and selecting the angle that achieved a reaction closest to the desired value. This procedure was carried out in Microsoft Excel, which allowed for the rapid evaluation of  $\alpha_3$  values. In order to determine the reaction for a given angle using Equation 4, the relative flow angle at station 2 had to be evaluated. This was done using the flow coefficient, the stage coefficient, and the relative flow angle at station 3 of the stage as shown in [4]:

$$\tan \beta_2 = \frac{\psi}{\varphi} - \tan \beta_3 \quad (5)$$

The reaction of the stage could then be evaluated using Equation 4 and the relative flow angles at station 2 and station 3. The reaction across the span of  $\alpha_3$  from  $0^\circ$ - $20^\circ$  in increments of  $1^\circ$  was calculated and the value of the absolute angle that gave the reaction closest to 50% was selected as the final absolute rotor angle to be used in the design.

### ***Flow Angles***

After the rotor absolute angle had been determined, the rest of the flow angles could be determined using the velocity triangles and the dimensionless numbers. The final angle to complete the velocity triangles was the nozzle absolute angle given by Equation 4.13b in [4]:

$$\tan \alpha_2 = \tan \beta_2 + \frac{1}{\varphi} \quad (6)$$

### ***Flow Velocities***

Once the flow coefficient has been determined, the axial velocity through the nozzle and the rotor can be calculated by rearranging Equation 2:

$$C_{x,1} = C_{x,2} = C_{x,3} = U * \varphi \quad (7)$$

With the axial velocity,  $C_x$ , measured in m/s. After the axial velocity had been calculated, the rest of the velocities could be determined from the velocity triangles. The nozzle absolute velocity is given by:

$$C_2 = \frac{C_{x,2}}{\cos \alpha_2} \quad (8)$$

Where the nozzle absolute velocity,  $C_2$ , is measured in m/s. Likewise, the rotor absolute velocity is given by the same trigonometric relation:

$$C_3 = \frac{C_{x,3}}{\cos \alpha_3} \quad (9)$$

From the velocity assumptions, the absolute inlet velocity is axial.

$$C_1 = C_{x,1} \quad (10)$$

The final velocities to calculate are the relative velocities at the nozzle and rotor. The nozzle relative velocity is determined from the velocity triangle:

$$w_2 = \frac{C_{x,2}}{\cos \beta_2} \quad (11)$$

The rotor relative velocity is calculated using the same relationship:

$$w_3 = \frac{C_{x,3}}{\cos \beta_3} \quad (12)$$

The determination of the velocities allowed for further design parameters of the turbine to be calculated based upon thermodynamic principles.

### ***Annulus Areas***

The central equation in determining the annulus areas is given on page 21 of [3]:

$$A = \frac{\dot{m}}{\rho * C_x} \quad (13)$$

Where  $A$ , the area, is in  $m^2$ ;  $\dot{m}$ , the constant mass flow rate through the turbine is in  $kg/s$ ;  $\rho$ , the density of the air at the temperature at the current station is in  $kg/m^3$ ; and the axial velocity,  $C_x$ , at the step is in  $m/s$ . The only unknown quantity in this equation is the density at the station being designed. Calculating the density requires employing several thermodynamic and isentropic flow relationships. The first step in calculating the density at station 1 and station 3 is to find the static temperature at the station. The design specifications [1] gave the stagnation temperature which is the temperature of the fluid if it were brought isentropically to rest. The static temperature can be calculated from the stagnation temperature assuming ideal gas behavior for air as shown on page 842 of [4]:

$$T = T_0 - \frac{C^2}{2 * c_p} \quad (14)$$

Where  $T$  is the static temperature in K,  $T_0$  is the stagnation temperature in K,  $C$  is the absolute velocity in  $m/s$ , and  $c_p$  is the specific heat capacity of air in  $J/kg \cdot K$ . The static temperature is the appropriate temperature to use to determine the pressure and density of the air at station 1 and 3. The pressure can then be calculated from the compressible flow relations as shown by equation 7.32 from [7]:

$$\frac{P}{P_0} = \left( \frac{T}{T_0} \right)^{\frac{\gamma}{\gamma-1}} \quad (15)$$

Where  $\gamma$  is the dimensionless ratio of specific heats and is equal to 1.333 for air at the operating temperatures of the turbine. The density at the station can be calculated from the ideal gas equation of state:

$$\rho = \frac{P}{R * T} \quad (16)$$

Where  $\rho$  is in  $kg/m^3$ ,  $P$  is in  $kPa$ ,  $R$ , the specific gas constant for air, is  $0.287 \text{ kJ/kg} \cdot K$ , and  $T$  is the static temperature in K. Finally, the annulus area at station 1, the inlet to the nozzle, can be calculated from Equation 13. The annulus area at station 3 can be calculated in the same manner.

Determining the annulus area at station 2 is not as straightforward because there are losses involved with the nozzle and therefore the flow is not isentropic. To account for the losses, the nozzle loss coefficient must be employed. This is given on page 22 of [3]:

$$\lambda_N = \frac{T_2 - T'_2}{\frac{C_2^2}{2 * c_p}} \quad (17)$$

Where  $\lambda_N$  is the dimensionless rotor loss coefficient,  $T_2$  is the static temperature in K, and  $T'_2$  is the isentropic static temperature in K. The isentropic static temperature is the temperature that would occur at station 2 if there were no losses in the nozzle. However, because there are losses, the actual temperature will be greater as kinetic energy is transformed into thermal energy. The correct temperature to use to evaluate the pressure at station 2 is therefore not the actual static temperature, but the isentropic static temperature,  $T'_2$ . The actual static temperature must be calculated using the definition of stagnation temperature as given in Equation 14. Once the actual static temperature has been determined, the isentropic static temperature is found through Equation 17. Then, the pressure at station 2 can be found using the same flow relation presented in Equation 15 rearranged to solve for  $P_2$ :

$$\frac{P_2}{P_{01}} = \left( \frac{T'_2}{T_{01}} \right)^{\gamma/(\gamma-1)} \quad (18)$$

Finally, the density at station 2 can be calculated from the actual static temperature at station 2,  $T_2$ , using the ideal gas equation of state (Equation 16). The annulus area at the exit of the stator is then determined. The area at station 2 is larger accounting for the nozzle losses than if the nozzle was isentropic because the pressure is reduced, which reduces the density and increases the needed area to pass the same mass flow of air.

### ***Diameters***

The three diameters required by [1] are the mean, hub, and tip diameters. The mean radius can be calculated from the mean blade speed as given on page 16 of [3]:

$$r_m = \frac{U}{\Omega * 2 * \pi} \quad (19)$$

Where  $U$  is the mean blade speed in m/s and  $\Omega$  is the rotational speed of the shaft in rev/sec. The mean radius could be calculated directly from the design specifications. The blade height,  $h$  (in m) can be determined from the area of the annulus (in m<sup>2</sup>) as shown on page 21 of [3]:

$$h = \frac{\Omega * A}{U} \quad (20)$$

The blade height of the nozzle reported is the average of the blades heights calculated using the area at station 1 and the area at station 2. Likewise, the blade height reported for the rotor row is the average of the blades heights found using the area at station 2 and the area at station 3. The blades are tapered axially as the area of the annulus increases moving through the turbine stage. The blade height is the difference between the hub and tip radii.:



$$h = r_t - r_h \quad (21)$$

Where  $r_t$  is the tip radius in m, and  $r_h$  is the hub radius in m. Moreover, the mean radius is the average of the tip and hub radii:

$$r_m = \frac{(r_t + r_h)}{2} \quad (22)$$

Rearranging Equations 21 and 22, it is possible to determine the tip radius:

$$r_t = r_m + \frac{h}{2} \quad (23)$$

The hub radius can then be found using a similar equation:

$$r_h = r_m - \frac{h}{2} \quad (24)$$

The hub and tip radii presented in the results are the average for the nozzle and for the rotor. Therefore, the nozzle results are the average of the radius at station 1 and the radius at station 2, while the rotor results are the average of the radius at station 2 and station 3.

### ***Number of Blades***

The last parameter to calculate was the number of blades. This required knowing the blade pitch, or the spacing between blades. However, before the pitch could be calculated, the axial chord of the blades first had to be calculated. The aspect ratio of a blade is defined on page 135 of [4]:

$$AR = \frac{h}{b} \quad (25)$$

Where AR is the dimensionless aspect ratio, h is the blade height in m, and b is the blade axial chord in m. The aspect ratio was not specified in the design parameters and was instead determined from the literature. According to page 135 of [4], a typical aspect ratio in a jet engine turbine is between 1 and 2. Based on the literature, an aspect ratio of 1.1 was selected for the design to minimize the number of blades and therefore the cost of the single stage turbine. The next step towards calculating the number of blades was to calculate the pitch from the Zweifel correlation. This empirical relationship between the blade pitch and the blade axial chord is designed to minimize losses across the stage. The equation for the Zweifel correlation is found on page 103 of [4]:

$$\frac{s}{b} = \frac{0.4}{\cos^2 \alpha_2 * (\tan \alpha_1 + \tan \alpha_2)} \quad (26)$$

This correlation allows the blade pitch,  $s$  (in m) to be calculated. Once the blade spacing has been determined, the number of blades could be determined from the mean blade radius and the spacing between the blades as shown on page 25 of [3]:

$$n = \frac{2 * \pi * r_m}{s} \quad (27)$$

The exact number of blades acquired from the calculation is rounded up to the nearest whole number to represent the physical consideration that the number of blades must be an integer.

### ***Work Output***

The work output of the turbine can be calculated from the definition of the stage loading coefficient (work coefficient) as shown on page 123 of [4]:

$$\dot{w} = \psi * U^2 = \dot{W} / \dot{m} \quad (28)$$

Where  $\dot{w}$  is the work rate per unit mass flow rate in  $\text{m}^2/\text{s}^2$ ,  $\psi$  is the unitless stage loading coefficient, and  $U$  is the mean blade speed in m/s. The work output can also be expressed in terms of the tangential absolute velocities,  $C_\theta$ , in what is known as the Euler work equation:

$$\dot{w} = U(C_{\theta,2} - C_{\theta,3}) \quad (29)$$

Where the absolute tangential velocities in m/s are in opposite directions which means that their magnitudes should be summed to arrive at the correct work output. The actual shaft work is found by multiplying  $\dot{w}$  by the mass flow rate of air through the turbine annulus and is measured in Watts ( $\text{kg} / \text{m}^2 \text{ s}^3$ ).

### ***Choke Condition at Nozzle Exit***

The air flow in the turbine should not become sonic, ( $\text{Mach} = 1$ ) because then the flow would become choked and shocks could occur in the turbine. To check that the flow is not sonic exiting the nozzle, the stagnation pressure ratio at the exit of the nozzle must be checked against the critical pressure ratio as shown in [7]:

$$\frac{P_{01}}{P_c} = \left( \frac{\gamma + 1}{2} \right)^{\frac{\gamma}{\gamma-1}} \quad (30)$$

The actual stagnation pressure ratio can be found from the stagnation to isentropic static temperature by rearranging Equation 18 from [7]:

$$\frac{P_{01}}{P_2} = \left( \frac{T_{01}}{T_2'} \right)^{\frac{\gamma}{\gamma-1}} \quad (31)$$

The actual pressure ratio must be less than the critical pressure ratio to prevent the condition of choked flow at the nozzle exit. If the flow is choked, then the exit absolute angle at station 3 or the flow coefficient needs to be adjusted to lower the pressure ratio.

### ***Mach Number Check***

The final step of the single stage turbine design was to ensure that the exit flow remained below the Mach number of 0.6 specified in the design requirements. The Mach number at the exit is the absolute velocity of the flow divided by the speed of sound at the temperature at station 3:

$$Ma_3 = \frac{C_3}{\sqrt{\gamma R T_3}} \quad (32)$$

If the Mach number was found to be in excess of the allowed value, the flow coefficient would have to be adjusted downward and the turbine redesigned.

### ***Isentropic Efficiency and Loss Coefficients***

After the turbine stage has been designed, the actual isentropic efficiency can be calculated. First, the actual nozzle and rotor energy loss coefficients must be determined. The loss coefficients can be calculated using the Soderberg correlation presented on page 100 of [4]:

$$\zeta^* = 0.04 + 0.06 \left( \frac{\varepsilon}{100} \right)^2 \quad (33)$$

Where  $\zeta^*$  is the loss coefficient and  $\varepsilon$  is a function of the deflection angles. For the nozzle:

$$\varepsilon = (\alpha_1 + \alpha_2) \quad (34)$$

Where the absolute angles are measured in degrees. For the rotor:

$$\varepsilon = (\beta_2 + \beta_3) \quad (35)$$

Where the relative angles are measured in degrees. The Soderberg correlation is valid for an aspect ratio of 3 and a Reynolds number of  $10^5$ . The calculated Reynold's number at station 2 was around  $4.3 * 10^5$  using properties for air from [8], which fit the correlation, but the chosen aspect ratio ( $h/b$ ) was below 3. Therefore, a correction factor to the energy loss coefficient must be used. The correction factor for the nozzle comes from page 100 of [4]:

$$\zeta_s = (1 + \zeta^*) * \left( 0.993 + 0.021 * \frac{b}{h} \right) - 1 \quad (36)$$

Where  $\zeta_s$  is the corrected energy loss coefficient and  $b/h$  is the inverse of the aspect ratio. The correction factor for the rotor takes the same form but with different empirical coefficients:

$$\zeta_R = (1 + \zeta^*) * \left(0.975 + 0.075 * \frac{b}{h}\right) - 1 \quad (37)$$

Once the nozzle energy loss coefficient and the rotor energy loss coefficient have been calculated, the overall isentropic efficiency of the turbine can be determined. The equation comes from page 128 of [4]:

$$\eta_{t,a} = \left[ 1 + \frac{T_{03}}{T_3} * \frac{\zeta_S * C_2^2 * \frac{T_3}{T_2} + w_3^2 * \zeta_R}{2 * c_p * (T_{01} - T_{03})} \right]^{-1} \quad (38)$$

The actual isentropic efficiency can then be compared to the design requirement for isentropic efficiency. If the actual efficiency is too low, the design will have to be altered to meet the required specifications.

### 3.3 Selection of Parameters

The complete listing of specified parameters is displayed in Section 4.1 in Table 3-Table 8.

The first parameter to select for the turbine was the flow coefficient,  $\phi$ . This was done using empirical data from Rolls Royce turbine testing as presented in Figure 4.11 of [4].

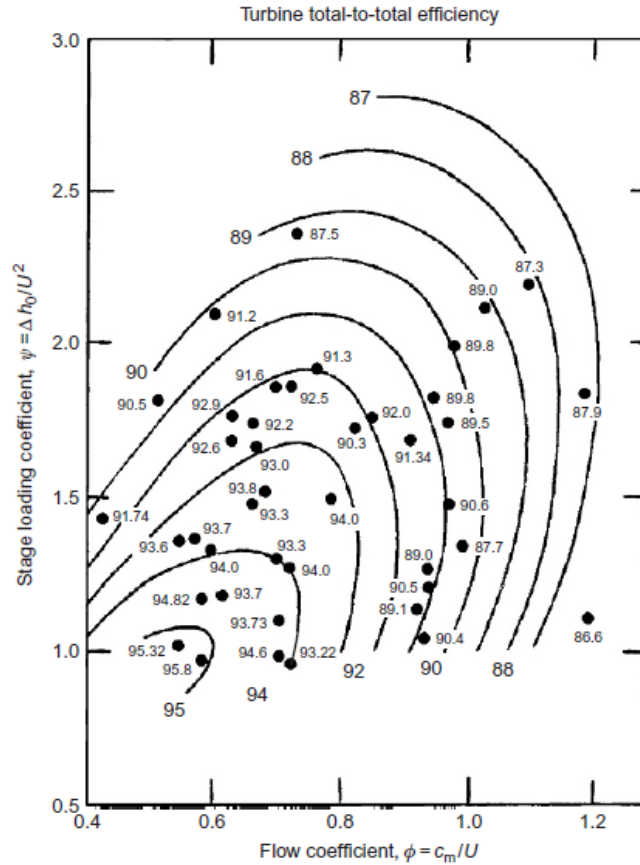


**Figure 3: Stage Loading Coefficient versus Flow Coefficient from [4]**

Figure 3 displays the stage loading coefficient versus the flow coefficient for varying isentropic efficiency contours. Because the desired isentropic efficiency was provided in the design specifications and the stage loading coefficient could be directly calculated from the design specifications, the flow coefficient was constrained based on this graph. The graph is constructed from data obtained from 70 Rolls-Royce aircraft gas turbines tested in 1965 in Derby, England. This data was assumed to be valid and the flow coefficient obtained from the data drove almost every other aspect of the turbine design. Although a closed form exact calculation for the flow coefficient would be preferable, the empirical correlation has been rigorously tested and has been shown to be an effective method on which to base the development of a turbine. With a stage loading coefficient of 1.44, and an isentropic efficiency of 0.91, a flow coefficient of 0.8 was selected from Figure 3.

After the flow coefficient had been determined, the absolute angle at station 3,  $\alpha_3$ , was the next parameter to specify. Although a multi-stage turbine generally has flow entering and exiting each stage axially, a single stage turbine is not constrained by the same limitation. Instead, the absolute angle at station 3 was chosen based on the design goal of achieving a 50% reaction. To that end, Microsoft Excel was used to calculate the reaction across a range of rotor exit angles using Equation 4 to determine which angle produced the reaction closest to 50%. The results of these calculations are shown in Figure 4. As can be seen, an absolute rotor exit angle of  $16^\circ$  results in an efficiency closest to 50 and therefore this was the angle selected for the turbine.

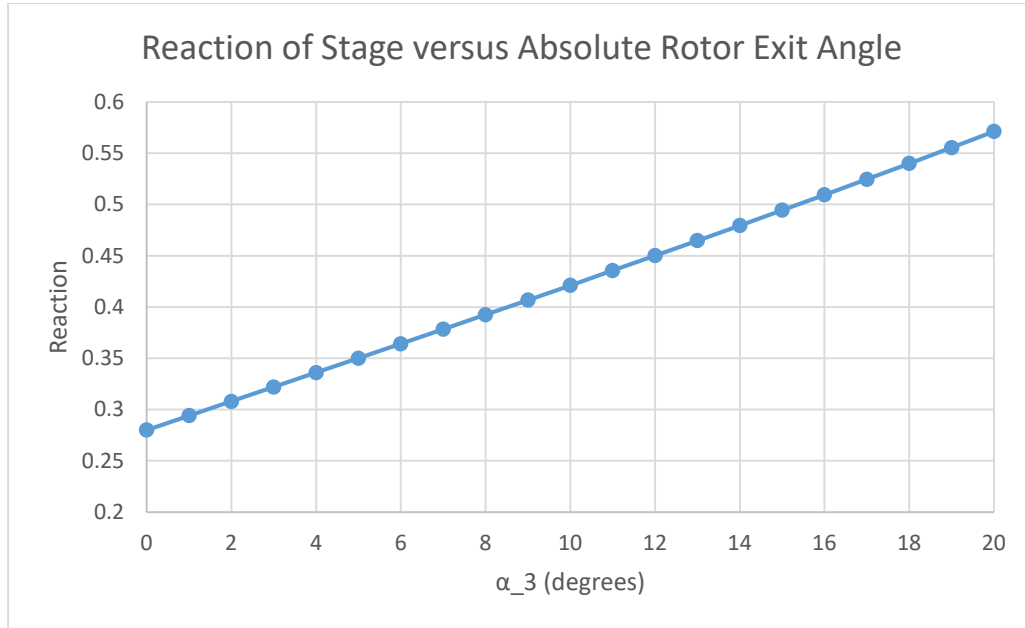


**Figure 4: Reaction of Stage versus Absolute Rotor Exit Angle**

After  $\alpha_3$  had been selected, the rest of the angles and velocities could be calculated from the dimensionless parameters and using the trigonometric relationships of the velocity triangles. Likewise, the annulus flow areas, tip and hub diameters, mean blade diameter, and blade height were completely set by the selected parameters and merely had to be calculated. The next design decision that had to be made was the aspect ratio, for the blades. This represents the ratio between the blade height and the axial chord of the blades. According to [3] and [4], an aspect ratio between 1 and 2 is typical for commercial jet engines. By altering the aspect ratio in Excel the effect on the number of stator and rotor blades could be observed. It was decided that the minimum number of blades that could be achieved would be ideal in order to minimize the manufacturing cost of the turbine. Based on the Excel calculations, it was determined that decreasing the aspect ratio lowered the number of blades in the turbine as demonstrated in Figure 5. After several iterations, the optimum aspect ratio between 1 and 2 was selected as 1.1. This minimized the number of blades while also staying between the boundaries presented in the literature and based on decades of design experience and experimental testing. Once the aspect ratio had been selected, the blade pitch could be determined from the Zweifel correlation, an

empirical relationship between the pitch of the blades, the blade axial chord, the absolute angle at station 1, and the absolute angle at station 2. After the blade pitch, or spacing between blades had been calculated, the number of blades could be determined. The exact number of blades obtained from Equation 30 was rounded up to the nearest whole number to determine the actual number of blades that would be needed in the stator row and in the rotor row.

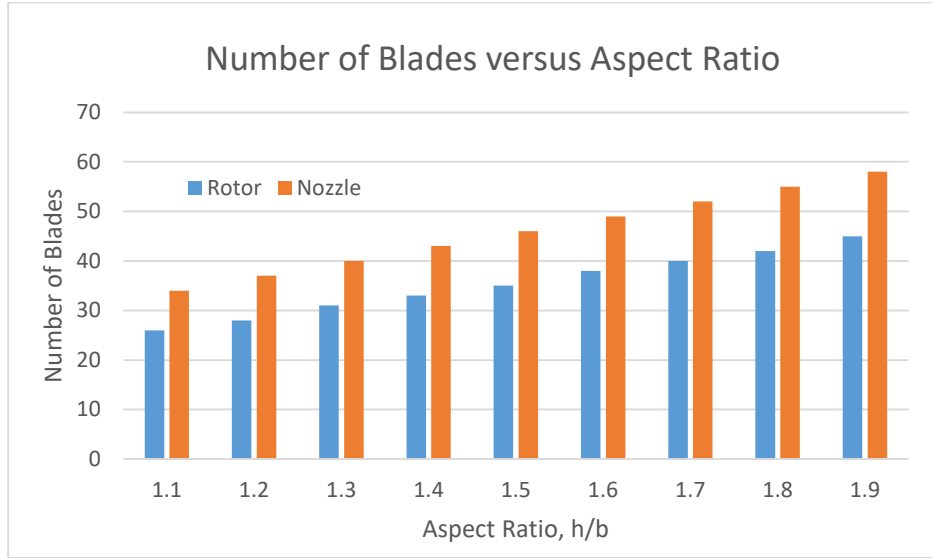


**Figure 5: Number of Blades versus Aspect Ratio**

The material for the blades was selected based on the graphs presented in [4]. The temperatures at all the stages were calculated based on compressible flow relationships and then the materials were evaluated based on their heat performance and cost. Blade cooling was determined to be out of the scope of the project, but could also be incorporated into the design as an additional safety factor and to prolong the service life of the blades.

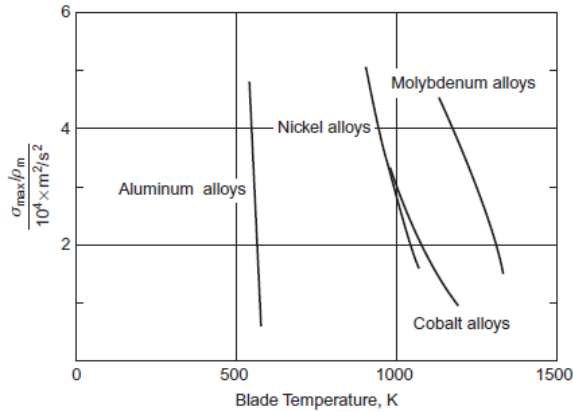


**Figure 6: Suitable Materials for Turbine Blades from [4]**

## Section 4: Results

### 4.1 Specifications

Parameter	Value
Stage loading (work) coefficient, $\psi$	1.430
Flow coefficient, $\phi$	0.8
Reaction, $R_N$	50.94 %
Exit Mach number, $Ma$	0.476
Number of stator blades	34
Number of rotor blades	26
Shaft work per unit mass flow rate, $\dot{w}$	166.46 kW
Work output of turbine, $\dot{W}$	3.3292 MW
Critical stagnation pressure ratio, $\frac{P_{01}}{P_c}$	1.852
Actual stagnation pressure ratio, $\frac{P_{01}}{P_2}$	1.027
Achieved Isentropic Efficiency	0.876

**Table 3: General Specifications**

Angle Description	Value
Absolute angle at nozzle inlet, $\alpha_1$	0°
Absolute angle at nozzle exit, $\alpha_2$	56.54°
Absolute angle at rotor exit, $\alpha_3$	16.0°
Absolute angle at nozzle exit, $\beta_2$	14.75°
Absolute angle at rotor exit, $\beta_3$	56.95°

**Table 4: Angle Specifications**



Velocity Description	Value (m/s)
Absolute velocity at station 1, $C_1$	272
Axial velocity at station 1, $C_{x,1}$	272
Absolute velocity at station 2, $C_2$	493.35
Axial velocity at station 2, $C_{x,2}$	272
Absolute Tangential velocity at station 2, $C_{\theta,2}$	411.59
Absolute velocity at station 3, $C_3$	282.96
Axial velocity at station 3, $C_{x,3}$	272
Absolute Tangential velocity at station 2, $C_{\theta,3}$	78.00
Relative velocity at station 2, $w_2$	281.26
Relative velocity at station 3, $w_3$	498.70

**Table 5: Velocity Specifications**

Area Description	Value (m <sup>2</sup> )
Area at station 1, $A_1$	0.0621
Area at station 2, $A_2$	0.0785
Area at station 3, $A_3$	0.1047

**Table 6: Area Specifications**

Dimension Description	Value (m)
Blade height at station 1, $h_1$	0.0456
Blade height at station 2, $h_2$	0.0577
Blade height at station 3, $h_3$	0.0770
Average Nozzle blade height, $h_s$	0.052
Average Rotor blade height, $h_r$	0.067
Mean radius, $r_m$	0.216
Average Nozzle Hub radius, $r_{h,s}$	0.191
Average Nozzle Tip radius, $r_{t,s}$	0.243
Average Rotor Hub radius, $r_{h,r}$	0.183
Average Rotor Tip radius, $r_{t,r}$	0.250

**Table 7: Dimension Specifications**

Blade Characteristic	Value
Aspect ratio, AR	1.1
Nozzle axial chord, $b_s$	0.0470 m
Rotor axial chord, $b_r$	0.0613 m
Nozzle blade pitch, $s_s$	0.0409 m
Rotor blade pitch, $s_r$	0.0533 m
Number of nozzle blades	34
Number of rotor blades	26

**Table 8: Blade Characteristic Specifications**

## 4.2 Velocity Triangles and Turbine Diagram

Pictured in Figure 7 are the velocity triangles for the final design. As can be seen, air flow enters the turbine stage axially but exits at a small absolute angle in order to achieve a reaction near 50%.

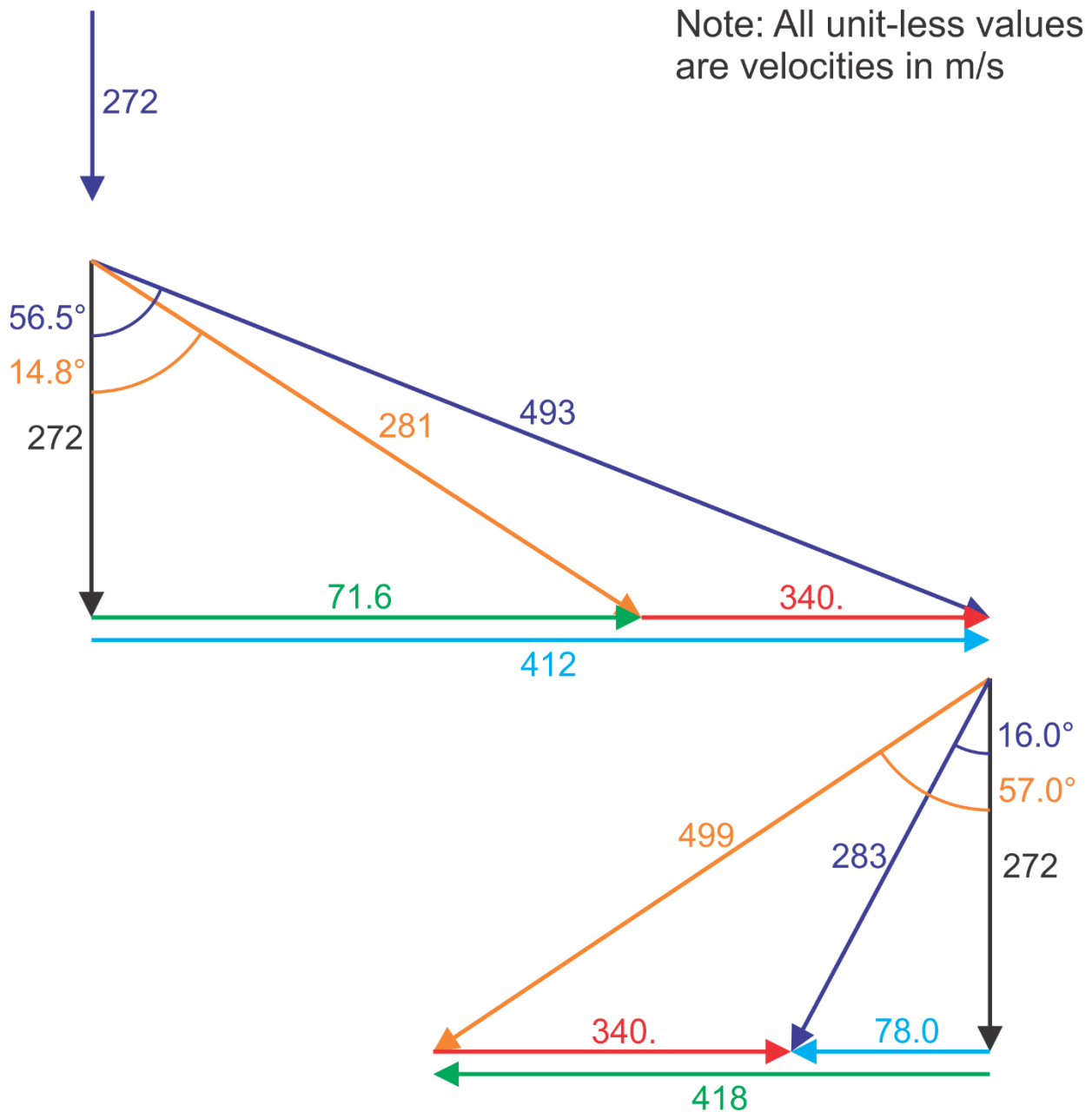
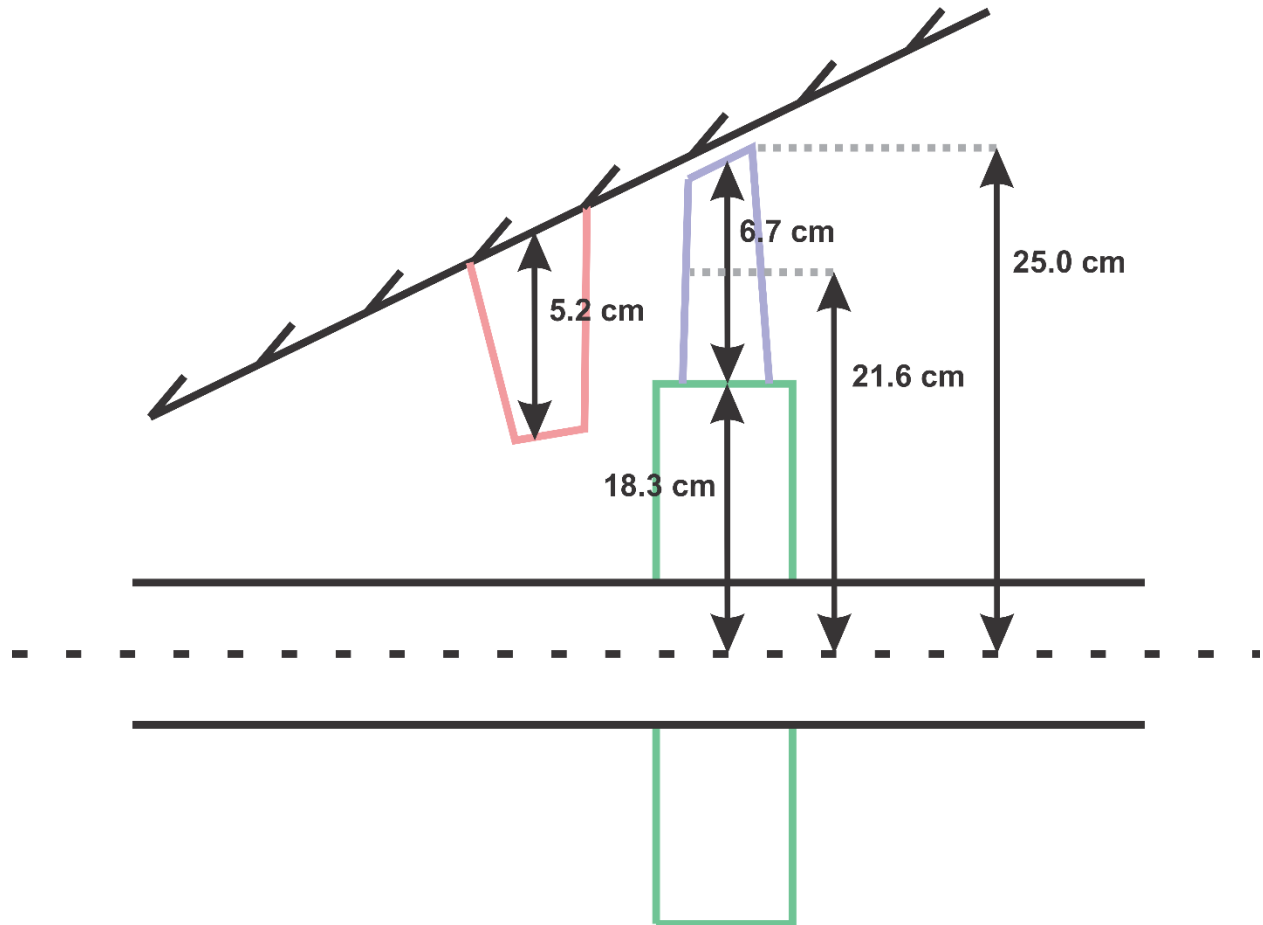


Figure 7: Velocity Triangles with Specification

### ***Turbine Dimensioned Diagram***

Pictured in Figure 8 is the turbine stage with appropriate dimensions. The dimensions for the blade heights and the hub and tip radii are the averages taken between the respective stations. For the full list of dimensions in the stage, refer to Table 7.



**Figure 8: Turbine Stage with Dimensions**

### 4.3 Bill of Materials and Cost Analysis

Item	Cost
All raw material (cobalt)	\$2600
Blade manufacturing	\$1200
Hub manufacturing	\$800
<b>Total</b>	<b>\$4600</b>

**Table 9: Bill of Materials (using [11], [13], [14])**

#### *Cost Analysis*

The blades in both the stator and the rotor will be cobalt, based on the heat that the blades will be subject to in the operation of the turbine stage. The material was selected by considering Figure 6 while also taking price and typical turbine blade materials into account. Cobalt should be able to withstand the operating temperatures even without advanced cooling methods typically employed in commercial turbines. Price estimates regarding the cost to manufacture do not include setup costs or fixed costs that would be incurred during the creation of the factory, but rather are steady-state costs given that the production process has stabilized. The turbine blades will be manufactured using investment casting; based on the mass of the cobalt per turbine, the unit cost will be around \$1,200 per turbine. Hub machining will need to be done to accommodate the turbine blades and tighter tolerances for rotation; this will require a 5-axis CNC mill. Between labor and tooling, the unit cost for the machined parts will be around \$800. Accounting for the cost of raw materials, the total unit cost for the turbine design is approximately \$4,600 [13][14].

Although it was not considered in this design, modern gas turbine engines use a thermal barrier coating to lower the temperature of metal surfaces. According to [12], thermal barrier coatings can increase efficiency, lower NO<sub>x</sub> emissions, and lead to greater thrust generation. However, the primary benefit of thermal barrier coatings is the extension of the life of the turbine blades. Turbine blades are subjected to extreme operating conditions and new coatings can double the life of the blades by increasing the capacity of the turbine blade to withstand heating. The first thermal barrier coatings, developed in the 1970s, were aluminide-based with ceramic coatings developed in subsequent years. The state of the art in thermal barrier coatings is electron beam physical vapor deposition applied yttria-stabilized zirconia as well as platinum modified diffusion aluminide. These modern coatings can reduce surface temperatures by up to 160°C when used in conjunction with external film and internal component air cooling as described in [12]. Although thermal barrier coatings were not used in this design, any turbine designed for the commercial market would need to incorporate this technology to be competitive. Any further

design work on this turbine should involve thermal barrier coatings as part of an adequate cooling system to increase the life of the engine and improve its performance characteristics.

## Section 5: Discussion

### 5.1 Design Justification

Three primary design decisions were made in the development of the single stage turbine. The first was the selection of the flow coefficient,  $\phi$ . This was done using empirical data presented in [4] and shown in Figure 3. The specific value of the flow coefficient was selected by calculating the stage loading coefficient,  $\psi$ , and choosing the flow coefficient that corresponded to the isentropic efficiency contour of 0.91. The design space of the turbine did not encompass varying flow coefficients, because unlike the absolute rotor exit angle, the flow coefficient was constrained based on the problem specifications and the empirical correlation.

The second important design consideration was the absolute rotor exit angle,  $\alpha_3$ . The determination of this angle was driven entirely by its effect on the reaction of the turbine. As stated previously, the design goal was for a reaction of 50%. According to the literature, namely [4] and [9], there are several advantages to a 50% reaction as compared to significantly higher or lower reactions. The primary is that the expansion of the air flow in the turbine is split evenly between the stator and the rotor. This leads to subsonic Mach numbers throughout the stage and improved performance through a variety of operating environments as the pressure losses that would occur through a shock wave are not present. Moreover, the equal distribution of pressure loss implied by a 50% reaction reduces the losses due to boundary layer separation and subsequent loss of stagnation pressure. For a fixed stage loading coefficient, there will be a reaction that maximizes the overall efficiency of the turbine stage as shown in Figure 8 from [4]. As the stage loading coefficient for the turbine based on the design specifications [1] was 1.44, the maximum efficiency will occur around a reaction of 50% which was consequently chosen as the objective for the turbine and determined the absolute rotor exit angle.

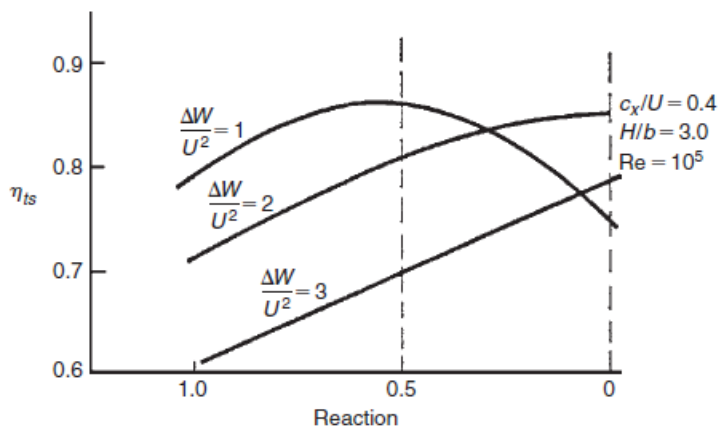


**Figure 9: Isentropic Efficiency versus Reaction for Fixed Values of Stage Loading Coefficient**

Another advantage of a 50% reaction is that the velocity triangles will be identical, and the blades in the stator and the rotor will be very similar meaning that manufacturing costs can be significantly reduced. Moreover, the design of the turbine will be greatly simplified if the velocity triangles are identical. Although this design did not have identical velocity triangles, the design was still aided by the similarity in the triangles and the blades themselves. Manufacturing costs were therefore decreased by designing for a reaction near 50%.

The final design choice that was left unconstrained by the problem statement was the aspect ratio of the blades. The aspect ratio is a measure of the blade height to the axial chord of the blade. According to [3] and [4], an aspect ratio of between 1 and 2 is typical for a small commercial turbojet turbine. As the aspect ratio is decreased, the number of blades decreases. However, [10] discusses one of the disadvantages of low aspect ratio turbines, namely the secondary flow losses that occur. Therefore, the aspect ratio for the turbine designed was not reduced below the acceptable range as determined by previous experience. In order to reduce manufacturing costs, a low aspect ratio of 1.1 was chosen for the single stage turbine as this minimized the number of blades required in the both the stator and the rotor while staying within the limits established by decades of turbine development.



## 5.2 Alternative Designs

The design space for the single stage turbine consisted of the range of absolute angles at station 3,  $\alpha_3$ , from 0 to 20°. Varying this angle changed the reaction of the turbine, and therefore, a span of angles was evaluated to determine which angle came closest to matching the design goal of a 50% reaction as discussed in Section 5.1. Table 10 shows the results of the calculations that were carried out in Microsoft Excel with the selected design angle highlighted.

$\alpha_3$ (degrees)	Rn
0	0.2800
1	0.2940
2	0.3080
3	0.3219
4	0.3360
5	0.3500
6	0.3641
7	0.3782
8	0.3924
9	0.4067
10	0.4211
11	0.4355
12	0.4501
13	0.4647
14	0.4795
15	0.4944
16	0.5094
17	0.5246
18	0.5400
19	0.5555
20	0.5712

**Table 10: Absolute Rotor Exit Angles and Corresponding Reactions**

Velocities, absolute and relative angles, and areas were calculated for the entire range of  $\alpha_3$ , but the absolute rotor exit angle of 16° was selected for the actual design as it best fit with the design goals. As the absolute rotor exit angle is increased, the reaction increases, which means that a greater portion of the total enthalpy drop of the turbine occurs in the rotor as shown in [4]:

$$R_N = \frac{h_{t,2} - h_{t,3}}{h_{t,1} - h_{t,3}} \quad (39)$$

This is in agreement with the theoretical predictions, because as the flow is turned through a greater angle at the rotor, a greater portion of the kinetic energy drop will occur in the rotor as compared to the nozzle. Both too large of an angle and too small of an angle resulted in off-design reactions, and these designs were discarded in favor of the optimal angle.

The other major design space that could be controlled was the aspect ratio of the blades. Based on the literature ([3] and [4]), typical aspect ratios for a commercial turbojet range between 1 and 2. As determined by these constraints, aspect ratios from 1 to 2 were evaluated in Excel to determine the effect on the number of blades required. The results of this process are shown in Table 11.

Aspect Ratio	Number of Rotor Blades	Number of Stator Blades
1.1	26	34
1.2	28	37
1.3	31	40
1.4	33	43
1.5	35	46
1.6	38	49
1.7	40	52
1.8	42	55
1.9	45	58

**Table 11: Span of Aspect Ratios and Corresponding Number of Blades**

As is demonstrated by the results, the lower the aspect ratio, the fewer required blades in both the stator and the rotor. This is because decreasing the aspect ratio, the ratio between the blade height and the axial chord of the blade increases the axial chord for a set blade height. The height of the blades had already been determined and therefore lowering the aspect ratio increased the axial chord. Subsequently, this increased the blade pitch, or spacing between blades by the Zweifel correlation from [3]:

$$\frac{s}{b} = \frac{0.4}{\cos^2 \alpha_2 * (\tan \alpha_1 + \tan \alpha_2)} \quad (40)$$

An increase in spacing between blades for a constant mean blade radius will decrease the number of blades in both the stator and rotor. Therefore, the aspect ratio was decreased to the lowest value while remaining within the limits determined through decades of turbine construction and operation.

## Section 6: Conclusion

---

A single stage turbine was designed for use in a small commercial turbojet engine. The requirements for the turbine were determined based on previous turbine design experience and cycle calculations for the engine. These specifications are outlined in their entirety in [1] with the most crucial aspects as follows: the turbine must operate at the same shaft speed, 250 rev/sec, as the compressor in the engine; the mean blade speed of the turbine is 340 m/s; the mass flow rate through the turbine is 20 kg/s of air, the isentropic efficiency for the overall turbine stage is 0.91; the estimated nozzle loss coefficient is 0.05; and the maximum exit Mach number is 0.6. The inlet stagnation temperature and the inlet stagnation pressure of the turbine were fixed from the cycle calculations for the engine as was the stagnation temperature drop and stagnation pressure ratio across the turbine stage.

The turbine was designed based on empirical data correlations as reported in [4] and a set of velocity triangles determined by the stated design goal of a 50% reaction. The flow coefficient for the turbine was selected based on experimental graphs to be 0.8 which meant that an absolute rotor exit angle,  $\alpha_3$ , of  $16^\circ$  resulted in a reaction near 50%. This angle selection drove the rest of the absolute and relative angles and velocities throughout the turbine, which ultimately constrained the physical dimensions for the turbine. The annulus area at station 1, the inlet to the nozzle, is  $0.0621 \text{ m}^2$ ; the annulus area at station 2, the exit of the nozzle and entrance to the rotor, is  $0.0785 \text{ m}^2$ ; and the annulus area at station 3, the exit of the rotor, is  $0.1047 \text{ m}^2$ . These areas subsequently determined the dimensions of the blades and the hub and tip diameters. The average nozzle blade height is 0.0510 m and the average rotor blade height is 0.0674 m. The mean radius is 0.216 m, the average nozzle hub radius is 0.191 m, the average nozzle tip radius is 0.242 m, the average rotor hub radius is 0.183 m, and the average rotor tip radius is 0.250 m. The final turbine design had a Mach number at the exit of the rotor of 0.476, below the maximum allowed. Moreover, the stagnation pressure ratio at the exit of the nozzle indicates that the flow remains subsonic throughout the turbine stage. The stator row has 34 blades and the rotor row has 26 blades. Accounting for the realized losses in the stator and the rotor, the isentropic efficiency of the final turbine design is 87.6% which was within an acceptable deviation from the requirements. The turbine blade material will be cobalt, and the blades will be manufactured using investment casting. The approximate cost to produce the blades in the turbine is \$4600. The turbine stage meets all the prescribed design requirements and produces a work output per unit mass flow rate of 166.460 kW/kg/s. Accounting for the 20 kg/s air mass flow rate in the problem specifications, the turbine will produce 3.329 MW of shaft work.

## Section 7: Acknowledgements

---

Our design team would like to thank the following individuals for their assistance with the design process. The single stage axial flow turbine design would not have been completed without their generous counsel.

**Professor Kadambi:** for describing a suggested method for the design process, for general all-around advice, for providing us with numerous invaluable references, and for being willing to answer our questions related to every aspect of the turbine design.

**Teaching Assistant Scott Rubeo:** for general assistance and for being willing to read and suggest improvements to an initial draft of this report.

## Section 8: References

---

- [1]. J. Kadambi, "Project #3 Design Requirements", EMAE 355 Class Documents, 2016.
- [2]. Fisher Scientific, "Cobalt Safety Data Sheet," Regulatory Affairs, 2015
- [3]. J. Kadambi, "Turbomachinery Notes and Suggested Design Procedure", EMAE 355 Lecture Notes, 2016.
- [4]. S. Dixon and C. Hall, *Fluid mechanics and thermodynamics of turbomachinery*, 6th ed. Burlington, MA: Butterworth-Heinemann/Elsevier, 2010.
- [5]. J. Kadambi, "Single Stage Axial Turbine Design", EMAE 355 Lecture, White Building 411, 2016.
- [6]. S. Turns, *Thermal-fluid Sciences: An Integrated Approach*. Cambridge: Cambridge University Press, 2006.
- [7]. J. Anderson, *Fundamentals of Aerodynamics*, 5th ed. Boston: McGraw-Hill, 2010.
- [8]. "Dry Air Properties", *Engineeringtoolbox.com*, 2016. [Online]. Available: [http://www.engineeringtoolbox.com/dry-air-properties-d\\_973.html](http://www.engineeringtoolbox.com/dry-air-properties-d_973.html). [Accessed: 15- Nov- 2016].
- [9]. S. Havakechian and R. Greim, "Aerodynamic design of 50 per cent reaction steam turbines", *Proceedings of the Institution of Mechanical Engineers, Part C: Journal of Mechanical Engineering Science*, vol. 213, no. 1, pp. 1-25, 1999.
- [10]. H. Orsan, "Investigation of Secondary Flow in Low Aspect Ratio Turbines using CFD", Royal Institute of Technology, Stockholm, 2014.
- [11]. "Cobalt", *Chemicool.com*, 2016. [Online]. Available: <http://www.chemicool.com/elements/cobalt.html>. [Accessed: 09- Nov- 2016].
- [12]. A. Feuerstein, J. Knapp, T. Taylor, A. Ashary, A. Bolcavage and N. Hitchman, "Technical and Economical Aspects of Current Thermal Barrier Coating Systems for Gas Turbine Engines by Thermal Spray and EBPVD: A Review", *Journal of Thermal Spray Technology*, vol. 17, no. 2, pp. 199-213, 2008.
- [13]. CustomPartNet, "Free injection molding, die and sand casting cost estimators," in *CustomPart*, 2009. [Online]. Available: <http://www.custompartnet.com/estimate/>. Accessed: Nov. 9, 2016.
- [14]. AFS Industrial Engineering Committee, "Cost estimating tips," in *American Foundry Society*. [Online]. Available: <http://www.afsinc.org/content.cfm?ItemNumber=6954>. Accessed: Nov. 9, 2016.

## Section 9: Academic Integrity Statement

---

This report was created by the group members listed below in compliance with Case Western Reserve University's Academic Integrity policy available at:

<https://students.case.edu/community/conduct/aiboard/policy.html>

By signing below, each group member is giving their affirmation to the above statement.

Name:

Signature:

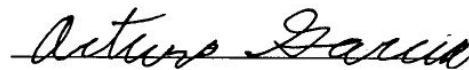
William Koehrsen



Tyler Eston



Arturo Garcia



Theodore Bastian



## Section 10: Appendices

---

### I: Sample Calculations for Final Design

Presented are the calculations for the final design. Numbers in the sample calculations may be in slight disagreement with the data tables provided in the report. Rounding errors in the calculations presented below are to blame for any discrepancy. For the final design, figures calculated in Excel were assumed to be correct and represent the described specifications.

Stage Loading Coefficient:

$$\psi = \frac{c_p * \Delta T_0}{U^2} = \frac{1148 * 145}{340^2} = 1.44$$

Flow coefficient (chosen from chart) with  $\psi$  and  $\eta_T$

$$\varphi = \frac{C_x}{U} = \frac{272}{340} = 0.8$$

Tangent of relative angle at station 3:

$$\tan \beta_3 = \tan \alpha_3 + \frac{1}{\varphi} = \tan 16 + \frac{1}{0.8} = 1.5367$$

Tangent of relative angle at station 2:

$$\tan \beta_2 = \frac{\psi}{\varphi} - \tan \beta_3 = \frac{1.44}{0.8} - 1.5367 = 0.263$$

Reaction with selected  $\alpha_3$  of  $16^\circ$

$$R_N = \frac{\varphi}{2} (\tan \beta_3 - \tan \beta_2) = \frac{0.8}{2} (1.5367 - 0.263) = 0.5094$$

Relative angle at station 3

$$\beta_3 = \tan^{-1} 1.5367 = 0.9939 \text{ rad}$$

Relative angle at station 2:

$$\beta_2 = \tan^{-1} 0.2632 = 0.2574 \text{ rad}$$

Absolute angle at station 2:

$$\tan \alpha_2 = \tan \beta_2 + \frac{1}{\varphi} = 0.2632 + \frac{1}{0.8} = 1.5312$$

$$\alpha_2 = \tan^{-1} 1.5312 = 0.9868 \text{ rad}$$

Absolute axial velocity:

$$C_{x,1} = C_{x,2} = C_{x,3} = U * \varphi = 340 * 0.8 = 272 \text{ m/s}$$

Absolute velocity at station 2:

$$C_2 = \frac{C_{x,2}}{\cos \alpha_2} = \frac{272}{\cos 0.9868} = 493.35 \text{ m/s}$$

Absolute velocity at station 3:

$$C_3 = \frac{C_{x,3}}{\cos \alpha_3} = \frac{272}{\cos 0.2793} = 282.96 \text{ m/s}$$

Absolute velocity at station 1:

$$C_1 = C_{x,1} = 272 \text{ m/s}$$

Relative velocity at station 2:

$$V_2 = \frac{C_{x,2}}{\cos \beta_2} = \frac{272}{\cos 0.2754} = 281.26 \text{ m/s}$$

Relative velocity at station 3:

$$V_3 = \frac{C_{x,3}}{\cos \beta_3} = \frac{272}{\cos 0.9939} = 498.7 \text{ m/s}$$

Annulus area:

$$A = \frac{\dot{m}}{\rho * C_x}$$

Static temperature:

$$T = T_0 - \frac{C^2}{2 * c_p}$$

Actual static temperature at station 2:

$$T_{02} - T_2 = \frac{C_2^2}{2 * c_p} = \frac{493.35^2}{2 * 1148} = 106.00 \text{ K}$$

$$T_2 = 1103.15 - 106.00 = 997.15 \text{ K}$$



Isentropic static temperature at station 2:

$$T_2 - T'_2 = \lambda_2 * (T_{02} - T_2) = 0.05 * 106.00 = 5.3 \text{ K}$$

$$T'_2 = T_2 - (T_2 - T'_2) = 997.15 - 5.3 = 991.8 \text{ K}$$

Stagnation pressure and stagnation temperature relationship:

$$\frac{P}{P_0} = \left( \frac{T}{T_0} \right)^{\frac{\gamma}{\gamma-1}}$$

Static pressure at station 2:

$$P_2 = P_{01} * \left( \frac{T'_2}{T_{01}} \right)^{\frac{\gamma}{\gamma-1}} = 410 * \left( \frac{991.8}{1103.15} \right)^{\frac{1.3333}{1.3333-1}} = 267.9 \text{ kPa}$$

Ideal gas equation of state:

$$\rho = \frac{P}{R * T}$$

Density at state 2:

$$\rho_2 = \frac{P_2}{R * T_2} = \frac{267.9}{0.287 * 997.15} = 0.9362 \text{ kg/m}^3$$

Annulus area at station 2:

$$A_2 = \frac{\dot{m}}{\rho_2 * c_{x2}} = \frac{20}{0.9362 * 272} = 0.0785 \text{ m}^2$$

Static temperature at station 1:

$$T_1 = T_{01} - \frac{c_1^2}{2 * c_p} = 1103.15 - \frac{272^2}{2 * 1148} = 1070.9 \text{ K}$$

Static pressure at station 1:

$$P_1 = \frac{P_{01}}{\left( \frac{T_{01}}{T_1} \right)^{\frac{\gamma}{\gamma-1}}} = \frac{410}{\left( \frac{1103.15}{1070.9} \right)^4} = 364.2 \text{ kPa}$$

Density at station 1:

$$\rho_1 = \frac{P_1}{R * T_1} = \frac{364.2}{0.287 * 1068.27} = 1.185 \text{ kg/m}^3$$

Annulus area at station 1:

$$A_1 = \frac{\dot{m}}{\rho_1 * c_{x1}} = \frac{20}{1.185 * 272} = 0.0621 \text{ m}^2$$

Temperature at station 3:

$$T_3 = T_{03} - \frac{c_3^2}{2 * c_p} = 958.15 - \frac{282.96^2}{2 * 1148} = 1068.3 \text{ K}$$

Pressure at station 3:

$$P_3 = P_{03} * \left(\frac{T_3}{T_{03}}\right)^{\frac{\gamma}{\gamma-1}} = 215.8 * \left(\frac{1068.3}{958.15}\right)^4 = 186.05 \text{ kPa}$$

Density at station 3:

$$\rho_3 = \frac{P_3}{R * T_3} = \frac{186.05}{0.287 * 1068.3} = 0.7021 \text{ kg/m}^3$$

Annulus area at station 3:

$$A_3 = \frac{\dot{m}}{\rho_3 * c_{x3}} = \frac{20}{0.7021 * 272} = 0.1047 \text{ m}^2$$

Blade height at station 1:

$$h_1 = A_1 * \frac{\Omega}{U} = 0.0601 * \frac{250}{340} = 0.0442 \text{ m}$$

Blade height at station 2:

$$h_2 = A_2 * \frac{\Omega}{U} = 0.0785 * \frac{250}{340} = 0.0577 \text{ m}$$

Blade height at station 3:

$$h_3 = A_3 * \frac{\Omega}{U} = 0.1047 * \frac{250}{340} = 0.0770 \text{ m}$$

Average Blade height of stator:

$$h_s = \frac{h_1 + h_2}{2} = \frac{0.0456 + 0.0577}{2} = 0.05165 \text{ m}$$

Average Blade height of rotor:

$$h_r = \frac{h_2 + h_3}{2} = \frac{0.0577 + 0.0770}{2} = 0.0674 \text{ m}$$

Mean radius:

$$r_m = \frac{U}{\Omega * 2 * \pi} = \frac{340}{250 * 2 * \pi}$$

Average Rotor Tip radius:

$$r_{t,r} = r_m + \frac{h_r}{2} = 0.216451 + \frac{0.0674}{2} = 0.2501 \text{ m}$$

Average Rotor Hub radius:

$$r_{h,r} = r_m - \frac{h_r}{2} = 0.2501 - \frac{0.0674}{2} = 0.1828 \text{ m}$$

Isentropic static temperature at station 3:

$$T'_3 = \frac{T_2}{(P_2/P_3)^\gamma} = \frac{997.1425}{(267.93/186.05)^{1.3333}} = 910.25 \text{ K}$$

Absolute tangential velocity at station 2:

$$c_{\theta 2} = c_{x2} * \tan \alpha_2 = 272 * \tan 0.9868 = 411.60 \text{ m/s}$$

Absolute tangential velocity at station 3:

$$c_{\theta 3} = c_{x3} * \tan \alpha_3 = 272 * \tan 0.2793 = 78.00 \text{ m/s}$$

Axial chord in stator:

$$b_2 = \frac{h_s}{h/b} = \frac{0.05165}{1.1} = 0.0470 \text{ m}$$

Axial chord in rotor:

$$b_3 = \frac{h_s}{h/b} = \frac{0.0674}{1.1} = 0.0613 \text{ m}$$

Zweifel correlation:

$$\frac{s}{b} = \frac{0.4}{\cos^2 \alpha_2 * (\tan \alpha_1 + \tan \alpha_2)}$$

Blade pitch (spacing) at station 2:

$$s_2 = b_2 * \frac{0.4}{\cos^2 \alpha_2 * (\tan \alpha_1 + \tan \alpha_2)} = 0.0470 * \frac{0.4}{\cos^2 0.9868 * (\tan 0 + \tan 0.9868)} = 0.0409 \text{ m}$$

Blade pitch (spacing) at station 3:

$$s_3 = b_3 * \frac{0.4}{\cos^2 \alpha_2 * (\tan \alpha_1 + \tan \alpha_2)} = 0.0613 * \frac{0.4}{\cos^2 0.9868 * (\tan 0 + \tan 0.9868)} = 0.0533 \text{ m}$$

Number of blades in stator row:

$$n_2 = \frac{2 * \pi * rm}{s_2} = \frac{2 * \pi * 0.216451}{0.0403} = 34 \text{ (rounded up to nearest whole number)}$$

Number of blades in rotor row:

$$n_3 = \frac{2 * \pi * rm}{s_3} = \frac{2 * \pi * 0.216451}{0.0613} = 26 \text{ (rounded up to whole number)}$$

Critical stagnation pressure ratio:

$$\frac{P_{01}}{P_c} = \left( \frac{\gamma + 1}{2} \right)^{\frac{\gamma}{\gamma - 1}} = \left( \frac{2.333}{2} \right)^4 = 1.852$$

Actual stagnation pressure ratio at station 2:

$$\frac{P_{01}}{P_2} = \left( \frac{T_{01}}{T'_2} \right)^{\frac{\gamma}{\gamma - 1}} = \left( \frac{1103.15}{991.84} \right)^4 = 1.530$$

Reynolds number at station 2:

$$Re_D = \frac{\rho * C_2 * D_h}{\mu} = \frac{0.353 * 493.35 * (0.0517 * 2)}{4.153 * 10^{-5}} = 4.34 * 10^5$$

Uncorrected nozzle energy loss coefficient:

$$\zeta^* = 0.04 + 0.06 \left( \frac{\varepsilon}{100} \right)^2 = 0.04 + 0.06 \left( \frac{0 + 56.54}{100} \right)^2 = 0.0592$$

Uncorrected rotor energy loss coefficient:

$$\zeta^* = 0.04 + 0.06 \left( \frac{\varepsilon}{100} \right)^2 = 0.04 + 0.06 \left( \frac{14.75 + 56.95}{100} \right)^2 = 0.0708$$

Corrected nozzle energy loss coefficient:

$$\zeta_S = (1 + \zeta^*) * \left(0.993 + 0.021 * \frac{b}{h}\right) - 1 = (1 + 0.0592) * (0.993 + 0.021 * 1.1^{-1}) - 1 = 0.072$$

Corrected rotor energy loss coefficient:

$$\zeta_R = (1 + \zeta^*) * \left(0.975 + 0.075 * \frac{b}{h}\right) - 1 = (1 + 0.0708) * (0.975 + 0.075 * 1.1^{-1}) - 1 = 0.117$$

Actual isentropic efficiency:

$$\eta_{t,a} = \left[ 1 + \frac{T_{03}}{T_3} * \frac{\zeta_S * C_2^2 * \frac{T_3}{T_2} + w_3^2 * \zeta_R}{2 * c_p * (T_{01} - T_{03})} \right]^{-1}$$

$$= \left[ 1 + \frac{958.2}{923.3} * \frac{0.072 * 493.35^2 * \frac{923.3}{997.1} + 498.7^2 * 0.117}{2 * 1148 * 145} \right]^{-1} = 0.876$$

Mach number at exit of rotor:

$$Ma_3 = \frac{C_3}{\sqrt{\gamma R T_3}} = \frac{282.96}{\sqrt{1.3333 * 287 * 923.28}} = 0.4760$$

Work output per unit mass flow rate:

$$\dot{w} = \psi * U^2 = 1.44 * 340^2 = 166460 \frac{m^2}{s^2} \left( \frac{Watts}{\frac{kg}{s}} \right)$$

Work output:

$$\dot{W} = \dot{w} * \dot{m} = 166340 \frac{Watts}{\frac{kg}{s}} * 20 \frac{kg}{s} = 3.32 MW$$

## II: Data Tables

$\alpha_3$ (degrees)	$\beta_2$	$\alpha_2$	$\beta_3$	$\alpha_3$ (radians)	Rn
0	0.5028	1.0637	0.8961	0.0000	0.2800
1	0.4893	1.0595	0.9028	0.0175	0.2940
2	0.4756	1.0553	0.9095	0.0349	0.3080
3	0.4617	1.0510	0.9160	0.0524	0.3219
4	0.4475	1.0467	0.9224	0.0698	0.3360
5	0.4332	1.0423	0.9288	0.0873	0.3500
6	0.4186	1.0377	0.9351	0.1047	0.3641
7	0.4037	1.0331	0.9412	0.1222	0.3782
8	0.3886	1.0285	0.9473	0.1396	0.3924
9	0.3732	1.0237	0.9534	0.1571	0.4067
10	0.3576	1.0188	0.9593	0.1745	0.4211
11	0.3416	1.0138	0.9652	0.1920	0.4355
12	0.3254	1.0086	0.9711	0.2094	0.4501
13	0.3089	1.0034	0.9769	0.2269	0.4647
14	0.2920	0.9980	0.9826	0.2443	0.4795
15	0.2749	0.9925	0.9883	0.2618	0.4944
16	0.2574	0.9868	0.9939	0.2793	0.5094
17	0.2395	0.9810	0.9995	0.2967	0.5246
18	0.2213	0.9750	1.0051	0.3142	0.5400
19	0.2028	0.9689	1.0106	0.3316	0.5555
20	0.1839	0.9625	1.0161	0.3491	0.5712

**Table 12: Angles**

$\alpha_3$ (degrees)	C_1 = Cx_1 (m/s)	Cx_2 (m/s)	C $\theta_2$	C_2 (m/s)	Cx_3 (m/s)	C $\theta_3$	C_3 (m/s)	V_2	V_3 (m/s)	Mach
0	272.00	272.00	489.59	560.07	272.00	0	272.00	310.42	435.41	0.46
1	272.04	272.00	484.84	555.93	272.00	4.74777766	272.04	308.16	439.13	0.46
2	272.17	272.00	480.09	551.79	272.00	9.498449302	272.17	305.96	442.87	0.46
3	272.37	272.00	475.33	547.65	272.00	14.25491596	272.37	303.81	446.63	0.46
4	272.66	272.00	470.57	543.52	272.00	19.02009285	272.66	301.72	450.42	0.46
5	273.04	272.00	465.79	539.39	272.00	23.79691648	273.04	299.68	454.24	0.46
6	273.50	272.00	461.00	535.26	272.00	28.58835199	273.50	297.70	458.08	0.46
7	274.04	272.00	456.19	531.13	272.00	33.39740057	274.04	295.78	461.96	0.46
8	274.67	272.00	451.36	526.98	272.00	38.22710704	274.67	293.91	465.88	0.46
9	275.39	272.00	446.51	522.83	272.00	43.08056777	275.39	292.11	469.82	0.46
10	276.20	272.00	441.63	518.67	272.00	47.96093875	276.20	290.37	473.81	0.46
11	277.09	272.00	436.72	514.50	272.00	52.87144409	277.09	288.68	477.84	0.47
12	278.08	272.00	431.77	510.31	272.00	57.81538477	278.08	287.06	481.91	0.47
13	279.15	272.00	426.79	506.10	272.00	62.79614799	279.15	285.51	486.03	0.47
14	280.33	272.00	421.77	501.87	272.00	67.81721677	280.33	284.03	490.20	0.47
15	281.60	272.00	416.71	497.62	272.00	72.88218034	281.60	282.61	494.42	0.47
16	282.9614	272.0000	411.5935	493.3490	272.0000	77.9947	282.9614	281.2643	498.7019	0.4760
17	284.43	272.00	406.43	489.05	272.00	83.15874536	284.43	279.99	503.04	0.48
18	286.00	272.00	401.21	484.72	272.00	88.37815738	286.00	278.80	507.44	0.48
19	287.67	272.00	395.93	480.36	272.00	93.65711081	287.67	277.69	511.90	0.48
20	289.46	272.00	390.59	475.97	272.00	98.99990372	289.46	276.66	516.43	0.49

**Table 13: Velocities**

$\alpha_3$ (degrees)	A_1 (m <sup>2</sup> )	A_2 (m <sup>2</sup> )	A_3 (m <sup>2</sup> )
0	0.0621	0.0869	0.1038
1	0.0621	0.0863	0.1038
2	0.0621	0.0857	0.1038
3	0.0621	0.0851	0.1039
4	0.0621	0.0846	0.1039
5	0.0621	0.0840	0.1039
6	0.0621	0.0835	0.1039
7	0.0621	0.0830	0.1040
8	0.0621	0.0825	0.1040
9	0.0621	0.0819	0.1041
10	0.0621	0.0814	0.1042
11	0.0621	0.0809	0.1042
12	0.0621	0.0805	0.1043
13	0.0621	0.0800	0.1044
14	0.0621	0.0795	0.1045
15	0.0621	0.0790	0.1046
16	0.0621	0.0785	0.1047
17	0.0621	0.0781	0.1048
18	0.0621	0.0776	0.1050
19	0.0621	0.0772	0.1051
20	0.0621	0.0767	0.1053

**Table 14: Annulus Areas**

				average stator	average rotor	stator	stator	rotor	rotor
				blade height	blade height	tip radius	hub radius	tip radius	hub radius
$\alpha_3$ (degrees)	h_1 (m)	h_2 (m)	h_3 (m)	h_s (m)	h_r (m)	rt_s (m)	rh_s (m)	rt_r (m)	rh_r (m)
0	0.0456	0.0639	0.0763	0.0547	0.0701	0.24382417	0.189077275	0.2515	0.1814
1	0.0456	0.0634	0.0763	0.0545	0.0699	0.243717149	0.189184296	0.2514	0.1815
2	0.0456	0.0630	0.0764	0.0543	0.0697	0.243612047	0.189289398	0.2513	0.1816
3	0.0456	0.0626	0.0764	0.0541	0.0695	0.243508769	0.189392677	0.2512	0.1817
4	0.0456	0.0622	0.0764	0.0539	0.0693	0.243407222	0.189494223	0.2511	0.1818
5	0.0456	0.0618	0.0764	0.0537	0.0691	0.24330732	0.189594125	0.2510	0.1819
6	0.0456	0.0614	0.0764	0.0535	0.0689	0.243208981	0.189692464	0.2509	0.1820
7	0.0456	0.0610	0.0765	0.0533	0.0687	0.243112127	0.189789318	0.2508	0.1821
8	0.0456	0.0606	0.0765	0.0531	0.0686	0.243016685	0.18988476	0.2507	0.1822
9	0.0456	0.0603	0.0765	0.0529	0.0684	0.242922584	0.189978861	0.2507	0.1823
10	0.0456	0.0599	0.0766	0.0528	0.0682	0.242829758	0.190071687	0.2506	0.1823
11	0.0456	0.0595	0.0766	0.0526	0.0681	0.242738144	0.190163301	0.2505	0.1824
12	0.0456	0.0592	0.0767	0.0524	0.0679	0.242647682	0.190253763	0.2504	0.1825
13	0.0456	0.0588	0.0768	0.0522	0.0678	0.242558314	0.190343131	0.2503	0.1826
14	0.0456	0.0584	0.0768	0.0520	0.0676	0.242469988	0.190431458	0.2503	0.1826
15	0.0456	0.0581	0.0769	0.0519	0.0675	0.242382651	0.190518795	0.2502	0.1827
16	0.0456	0.0577	0.0770	0.0517	0.0674	0.2423	0.1906	0.2501	0.1828
17	0.0456	0.0574	0.0771	0.0515	0.0673	0.242210752	0.190690693	0.2501	0.1828
18	0.0456	0.0571	0.0772	0.0514	0.0671	0.242126102	0.190775344	0.2500	0.1829
19	0.0456	0.0567	0.0773	0.0512	0.0670	0.242042261	0.190859185	0.2500	0.1829
20	0.0456	0.0564	0.0774	0.0510	0.0669	0.24195919	0.190942255	0.2499	0.1830

**Table 15: Blade Dimensions**

	Axial Chord		Blade Pitch		Number of blades		Rotor Loss Coefficient
$\alpha_3$ (degrees)	b2	b3	s2	s3	n2	n3	$\lambda_R$
0	0.0498	0.0637	0.0469	0.0600	30	23	0.138745972
1	0.0496	0.0635	0.0465	0.0596	30	23	0.137707111
2	0.0494	0.0633	0.0461	0.0591	30	24	0.136649693
3	0.0492	0.0632	0.0456	0.0586	30	24	0.13557475
4	0.0490	0.0630	0.0452	0.0582	31	24	0.134483194
5	0.0488	0.0628	0.0449	0.0577	31	24	0.133375819
6	0.0487	0.0627	0.0445	0.0573	31	24	0.132253317
7	0.0485	0.0625	0.0441	0.0568	31	24	0.131116287
8	0.0483	0.0623	0.0437	0.0564	32	25	0.129965239
9	0.0481	0.0622	0.0433	0.0560	32	25	0.1288006
10	0.0480	0.0620	0.0430	0.0556	32	25	0.127622727
11	0.0478	0.0619	0.0426	0.0552	32	25	0.126431906
12	0.0476	0.0618	0.0422	0.0548	33	25	0.12522836
13	0.0475	0.0616	0.0419	0.0544	33	26	0.124012251
14	0.0473	0.0615	0.0415	0.0540	33	26	0.122783688
15	0.0471	0.0614	0.0412	0.0536	34	26	0.121542726
16.0000	0.0470	0.0613	0.0409	0.0533	34	26	0.1203
17	0.0468	0.0611	0.0405	0.0529	34	26	0.119023589
18	0.0467	0.0610	0.0402	0.0526	34	26	0.117745293
19	0.0465	0.0609	0.0399	0.0522	35	27	0.11645436
20	0.0464	0.0608	0.0396	0.0519	35	27	0.115150627

**Table 16: Blade Characteristics**





# Fisher Scientific

Part of Thermo Fisher Scientific

## SAFETY DATA SHEET

Creation Date 18-Oct-2010

Revision Date 16-Apr-2015

Revision Number 2

### 1. Identification

**Product Name** Cobalt, powder

**Cat No. :** C363-100

**Synonyms** Color Index No. 77320.

**Recommended Use** Laboratory chemicals.

**Uses advised against** No Information available

**Details of the supplier of the safety data sheet**

**Company**

Fisher Scientific  
One Reagent Lane  
Fair Lawn, NJ 07410  
Tel: (201) 796-7100

**Emergency Telephone Number**

CHEMTREC®, Inside the USA: 800-424-9300  
CHEMTREC®, Outside the USA: 001-703-527-3887

### 2. Hazard(s) identification

**Classification**

This chemical is considered hazardous by the 2012 OSHA Hazard Communication Standard (29 CFR 1910.1200)

Flammable solids	Category 2
Acute oral toxicity	Category 4
Acute Inhalation Toxicity - Dusts and Mists	Category 1
Serious Eye Damage/Eye Irritation	Category 2
Respiratory Sensitization	Category 1
Skin Sensitization	Category 1
Carcinogenicity	Category 1B
Reproductive Toxicity	Category 1A
Specific target organ toxicity (single exposure)	Category 3
Target Organs - Respiratory system, Central nervous system (CNS).	
Specific target organ toxicity - (repeated exposure)	Category 2
Target Organs - Liver, Kidney.	
Combustible dust	Yes

**Label Elements**

**Signal Word**

Danger

**Hazard Statements**

Flammable solid May form combustible dust concentrations in air  
Harmful if swallowed

May cause an allergic skin reaction  
Causes serious eye irritation  
Fatal if inhaled  
May cause allergy or asthma symptoms or breathing difficulties if inhaled  
May cause respiratory irritation  
May cause drowsiness or dizziness  
May cause cancer by inhalation  
May damage fertility or the unborn child  
May cause damage to organs through prolonged or repeated exposure



### Precautionary Statements

#### Prevention

Obtain special instructions before use  
Do not handle until all safety precautions have been read and understood  
Use personal protective equipment as required  
Wash face, hands and any exposed skin thoroughly after handling  
Do not eat, drink or smoke when using this product  
Do not breathe dust/fume/gas/mist/vapors/spray  
Use only outdoors or in a well-ventilated area  
Wear respiratory protection  
In case of inadequate ventilation wear respiratory protection  
Contaminated work clothing should not be allowed out of the workplace  
Keep away from heat/sparks/open flames/hot surfaces. - No smoking  
Ground/bond container and receiving equipment  
Use explosion-proof electrical/ventilating/lighting/equipment  
Wear protective gloves/protective clothing/eye protection/face protection

#### Response

IF exposed or concerned: Get medical attention/advice

#### Inhalation

IF INHALED: Remove victim to fresh air and keep at rest in a position comfortable for breathing  
Immediately call a POISON CENTER or doctor/physician

#### Skin

IF ON SKIN: Wash with plenty of soap and water  
If skin irritation or rash occurs: Get medical advice/attention  
Wash contaminated clothing before reuse

#### Eyes

IF IN EYES: Rinse cautiously with water for several minutes. Remove contact lenses, if present and easy to do. Continue rinsing  
If eye irritation persists: Get medical advice/attention

#### Ingestion

IF SWALLOWED: Call a POISON CENTER or doctor/physician if you feel unwell  
Rinse mouth

#### Fire

In case of fire: Use CO<sub>2</sub>, dry chemical, or foam for extinction

#### Storage

Store locked up  
Store in a well-ventilated place. Keep container tightly closed

#### Disposal

Dispose of contents/container to an approved waste disposal plant

#### Hazards not otherwise classified (HNOC)

Very toxic to aquatic life with long lasting effects  
May form combustible dust concentrations in air

### 3. Composition / information on ingredients

Component	CAS-No	Weight %
Cobalt, powder	7440-48-4	>95

### 4. First-aid measures

<b>General Advice</b>	Show this safety data sheet to the doctor in attendance. Immediate medical attention is required.
<b>Eye Contact</b>	Rinse immediately with plenty of water, also under the eyelids, for at least 15 minutes. In the case of contact with eyes, rinse immediately with plenty of water and seek medical advice.
<b>Skin Contact</b>	Wash off immediately with plenty of water for at least 15 minutes. Immediate medical attention is required.
<b>Inhalation</b>	Move to fresh air. If breathing is difficult, give oxygen. Do not use mouth-to-mouth resuscitation if victim ingested or inhaled the substance; induce artificial respiration with a respiratory medical device. Immediate medical attention is required.
<b>Ingestion</b>	Do not induce vomiting. Call a physician or Poison Control Center immediately.
<b>Most important symptoms/effects</b>	May cause allergy or asthma symptoms or breathing difficulties if inhaled. May cause allergic skin reaction. . Symptoms of allergic reaction may include rash, itching, swelling, trouble breathing, tingling of the hands and feet, dizziness, lightheadedness, chest pain, muscle pain or flushing
<b>Notes to Physician</b>	Treat symptomatically

### 5. Fire-fighting measures

**Unsuitable Extinguishing Media** No information available

**Flash Point** Not applicable  
**Method -** No information available

**Autoignition Temperature**

**Explosion Limits**

**Upper** No data available  
**Lower** No data available  
**Sensitivity to Mechanical Impact** No information available  
**Sensitivity to Static Discharge** No information available

#### Specific Hazards Arising from the Chemical

Flammable. Containers may explode when heated. Dust can form an explosive mixture in air. Do not allow run-off from fire fighting to enter drains or water courses.

#### Hazardous Combustion Products

Cobalt oxides.

#### Protective Equipment and Precautions for Firefighters

As in any fire, wear self-contained breathing apparatus pressure-demand, MSHA/NIOSH (approved or equivalent) and full protective gear. Thermal decomposition can lead to release of irritating gases and vapors.

#### NFPA

**Health**  
4

**Flammability**  
3

**Instability**  
0

**Physical hazards**  
N/A

### 6. Accidental release measures

**Personal Precautions** Use personal protective equipment. Ensure adequate ventilation. Avoid dust formation.

**Environmental Precautions** Evacuate personnel to safe areas. Keep people away from and upwind of spill/leak. Do not flush into surface water or sanitary sewer system. Do not allow material to contaminate ground water system. Prevent product from entering drains. Local authorities should be advised if significant spillages cannot be contained. Should not be released into the environment. See Section 12 for additional ecological information. Avoid release to the environment. Collect spillage.

**Methods for Containment and Clean Up** Avoid dust formation. Sweep up or vacuum up spillage and collect in suitable container for disposal.

## 7. Handling and storage

**Handling** Wear personal protective equipment. Do not get in eyes, on skin, or on clothing. Avoid dust formation. Use only under a chemical fume hood. Do not breathe vapors/dust. Do not ingest.

**Storage** Keep containers tightly closed in a dry, cool and well-ventilated place.

## 8. Exposure controls / personal protection

### Exposure Guidelines

Component	ACGIH TLV	OSHA PEL	NIOSH IDLH
Cobalt, powder	TWA: 0.02 mg/m <sup>3</sup>	(Vacated) TWA: 0.05 mg/m <sup>3</sup> TWA: 0.1 mg/m <sup>3</sup>	IDLH: 20 mg/m <sup>3</sup> TWA: 0.05 mg/m <sup>3</sup>

Component	Quebec	Mexico OEL (TWA)	Ontario TWAEV
Cobalt, powder	TWA: 0.02 mg/m <sup>3</sup>	TWA: 0.1 mg/m <sup>3</sup>	TWA: 0.02 mg/m <sup>3</sup>

### Legend

ACGIH - American Conference of Governmental Industrial Hygienists

OSHA - Occupational Safety and Health Administration

NIOSH IDLH: The National Institute for Occupational Safety and Health Immediately Dangerous to Life or Health

**Engineering Measures** Ensure that eyewash stations and safety showers are close to the workstation location. Ensure adequate ventilation, especially in confined areas. Use explosion-proof electrical/ventilating/lighting/equipment.

### Personal Protective Equipment

**Eye/face Protection** Wear appropriate protective eyeglasses or chemical safety goggles as described by OSHA's eye and face protection regulations in 29 CFR 1910.133 or European Standard EN166. Tightly fitting safety goggles.

**Skin and body protection** Long sleeved clothing.

**Respiratory Protection** Follow the OSHA respirator regulations found in 29 CFR 1910.134 or European Standard EN 149. Use a NIOSH/MSHA or European Standard EN 149 approved respirator if exposure limits are exceeded or if irritation or other symptoms are experienced.

**Hygiene Measures** Handle in accordance with good industrial hygiene and safety practice.

## 9. Physical and chemical properties

<b>Physical State</b>	Solid
<b>Appearance</b>	Grey
<b>Odor</b>	Odorless
<b>Odor Threshold</b>	No information available
<b>pH</b>	No information available
<b>Melting Point/Range</b>	1495 °C / 2723 °F
<b>Boiling Point/Range</b>	2870 °C / 5198 °F @ 760 mmHg

Flash Point	Not applicable
Evaporation Rate	Not applicable
Flammability (solid,gas)	No information available
Flammability or explosive limits	
Upper	No data available
Lower	No data available
Vapor Pressure	No information available
Vapor Density	Not applicable
Relative Density	No information available
Solubility	Insoluble in water
Partition coefficient; n-octanol/water	No data available
Autoignition Temperature	
Decomposition Temperature	No information available
Viscosity	Not applicable
Molecular Formula	Co
Molecular Weight	58.93

## 10. Stability and reactivity

Reactive Hazard	Yes
Stability	Stable under normal conditions.
Conditions to Avoid	Incompatible products. Excess heat.
Incompatible Materials	Strong oxidizing agents, Strong acids
Hazardous Decomposition Products	Cobalt oxides
Hazardous Polymerization	Hazardous polymerization does not occur.
Hazardous Reactions	None under normal processing.

## 11. Toxicological information

### Acute Toxicity

#### Product Information

##### Component Information

Component	LD50 Oral	LD50 Dermal	LC50 Inhalation
Cobalt, powder	6170 mg/kg ( Rat )	Not listed	10 mg/L ( Rat ) 1 h

**Toxicologically Synergistic** No information available

#### Products

#### Delayed and immediate effects as well as chronic effects from short and long-term exposure

Irritation	No information available
Sensitization	No information available

**Carcinogenicity** Cobalt has not been shown to be carcinogenic to humans. The National Toxicology Program (NTP) does not recognize cobalt as an animal or human carcinogen. This product is a cobalt containing compound. The International Agency for Research on Cancer (IARC) classifies cobalt as "possibly carcinogenic" to human (IARC 2B) based on animal studies. Refer to IARC website ([www.iarc.fr](http://www.iarc.fr)) for most recent information. ACGIH (American Conference of Governmental Industrial Hygienist) has given Cobalt and Cobalt Inorganic Compounds a rating of A3, animal carcinogen. ACGIH states that available epidemiologic studies do not confirm an increased risk of cancer in exposed humans. The table below indicates whether each agency has listed any ingredient as a carcinogen.

Component	CAS-No	IARC	NTP	ACGIH	OSHA	Mexico
Cobalt, powder	7440-48-4	Group 2B	Not listed	A3	X	A3

IARC: (International Agency for Research on Cancer)

ACGIH: (American Conference of Governmental Industrial Hygienists)

Mexico - Occupational Exposure Limits - Carcinogens

IARC: (International Agency for Research on Cancer)

Group 1 - Carcinogenic to Humans

Group 2A - Probably Carcinogenic to Humans

Group 2B - Possibly Carcinogenic to Humans

A1 - Known Human Carcinogen

A2 - Suspected Human Carcinogen

A3 - Animal Carcinogen

ACGIH: (American Conference of Governmental Industrial Hygienists)

Mexico - Occupational Exposure Limits - Carcinogens

A1 - Confirmed Human Carcinogen

A2 - Suspected Human Carcinogen

A3 - Confirmed Animal Carcinogen

A4 - Not Classifiable as a Human Carcinogen

A5 - Not Suspected as a Human Carcinogen

<b>Mutagenic Effects</b>	In vitro tests have shown mutagenic effects
<b>Reproductive Effects</b>	No information available.
<b>Developmental Effects</b>	No information available.
<b>Teratogenicity</b>	No information available.
<b>STOT - single exposure</b>	Respiratory system Central nervous system (CNS)
<b>STOT - repeated exposure</b>	Liver Kidney
<b>Aspiration hazard</b>	No information available
<b>Symptoms / effects, both acute and delayed</b>	Symptoms of allergic reaction may include rash, itching, swelling, trouble breathing, tingling of the hands and feet, dizziness, lightheadedness, chest pain, muscle pain or flushing
<b>Endocrine Disruptor Information</b>	No information available
<b>Other Adverse Effects</b>	See actual entry in RTECS for complete information.

## 12. Ecological information

### Ecotoxicity

Very toxic to aquatic organisms, may cause long-term adverse effects in the aquatic environment. The product contains following substances which are hazardous for the environment. May cause long-term adverse effects in the environment. Do not allow material to contaminate ground water system.

Component	Freshwater Algae	Freshwater Fish	Microtox	Water Flea
Cobalt, powder	Not listed	100 mg/L LC50 96 h	Not listed	Not listed

**Persistence and Degradability** Insoluble in water May persist

**Bioaccumulation/ Accumulation** No information available.

**Mobility** Is not likely mobile in the environment due its low water solubility.

## 13. Disposal considerations

**Waste Disposal Methods** Chemical waste generators must determine whether a discarded chemical is classified as a hazardous waste. Chemical waste generators must also consult local, regional, and national hazardous waste regulations to ensure complete and accurate classification.

## 14. Transport information

### DOT

<b>UN-No</b>	UN3089
<b>Proper Shipping Name</b>	METAL POWDERS, FLAMMABLE, N.O.S.
<b>Proper technical name</b>	(Cobalt)
<b>Hazard Class</b>	4.1
<b>Packing Group</b>	III

### TDG

<b>UN-No</b>	UN3089
--------------	--------

Proper Shipping Name	METAL POWDERS, FLAMMABLE, N.O.S.
Hazard Class	4.1
Packing Group	III
<b>IATA</b>	
UN-No	UN3089
Proper Shipping Name	METAL POWDER, FLAMMABLE, N.O.S.
Hazard Class	4.1
Packing Group	II
<b>IMDG/IMO</b>	
UN-No	UN3089
Proper Shipping Name	METAL POWDER, FLAMMABLE, N.O.S.
Hazard Class	4.1
Packing Group	II

## 15. Regulatory information

### International Inventories

Component	TSCA	DSL	NDSL	EINECS	ELINCS	NLP	PICCS	ENCS	AICS	IECSC	KECL
Cobalt, powder	X	X	-	231-158-0	-		X	-	X	X	X

#### Legend:

X - Listed

E - Indicates a substance that is the subject of a Section 5(e) Consent order under TSCA.

F - Indicates a substance that is the subject of a Section 5(f) Rule under TSCA.

N - Indicates a polymeric substance containing no free-radical initiator in its inventory name but is considered to cover the designated polymer made with any free-radical initiator regardless of the amount used.

P - Indicates a commenced PMN substance

R - Indicates a substance that is the subject of a Section 6 risk management rule under TSCA.

S - Indicates a substance that is identified in a proposed or final Significant New Use Rule

T - Indicates a substance that is the subject of a Section 4 test rule under TSCA.

XU - Indicates a substance exempt from reporting under the Inventory Update Rule, i.e. Partial Updating of the TSCA Inventory Data Base Production and Site Reports (40 CFR 710(B)).

Y1 - Indicates an exempt polymer that has a number-average molecular weight of 1,000 or greater.

Y2 - Indicates an exempt polymer that is a polyester and is made only from reactants included in a specified list of low concern reactants that comprises one of the eligibility criteria for the exemption rule.

### U.S. Federal Regulations

TSCA 12(b) Not applicable

### SARA 313

Component	CAS-No	Weight %	SARA 313 - Threshold Values %
Cobalt, powder	7440-48-4	>95	0.1

### SARA 311/312 Hazardous Categorization

Acute Health Hazard	Yes
Chronic Health Hazard	Yes
Fire Hazard	Yes
Sudden Release of Pressure Hazard	No
Reactive Hazard	Yes

Clean Water Act Not applicable

### Clean Air Act

Component	HAPS Data	Class 1 Ozone Depletors	Class 2 Ozone Depletors
Cobalt, powder	X		-

OSHA Occupational Safety and Health Administration  
Not applicable

### CERCLA

Not applicable

**California Proposition 65**

This product contains the following Proposition 65 chemicals:

Component	CAS-No	California Prop. 65	Prop 65 NSRL	Category
Cobalt, powder	7440-48-4	Carcinogen	-	Carcinogen

**State Right-to-Know**

Component	Massachusetts	New Jersey	Pennsylvania	Illinois	Rhode Island
Cobalt, powder	X	X	X	X	X

**U.S. Department of Transportation**

Reportable Quantity (RQ): N  
DOT Marine Pollutant N  
DOT Severe Marine Pollutant N

**U.S. Department of Homeland Security**

This product does not contain any DHS chemicals.

**Other International Regulations****Mexico - Grade**

No information available

**Canada**

This product has been classified in accordance with the hazard criteria of the Controlled Products Regulations (CPR) and the MSDS contains all the information required by the CPR

**WHMIS Hazard Class**

B4 Flammable solid  
D2A Very toxic materials  
D1A Very toxic materials

**16. Other information****Prepared By**

Regulatory Affairs  
Thermo Fisher Scientific  
Email: EMSDS.RA@thermofisher.com

**Creation Date**

18-Oct-2010

**Revision Date**

16-Apr-2015

**Print Date**

16-Apr-2015

**Revision Summary**

This document has been updated to comply with the US OSHA HazCom 2012 Standard replacing the current legislation under 29 CFR 1910.1200 to align with the Globally Harmonized System of Classification and Labeling of Chemicals (GHS); SDS sections updated; 2; 15

**Disclaimer**

The information provided on this Safety Data Sheet is correct to the best of our knowledge, information and belief at the date of its publication. The information given is designed only as a guide for safe handling, use, processing, storage, transportation, disposal and release and is not to be considered as a warranty or quality specification. The information relates only to the specific material designated and may not be valid for such material used in combination with any other material or in any process, unless specified in the text.

**End of SDS**